# Final report to the Earthquake Commission on Project BI 10/603,

# Time-varying seismic velocity in New Zealand's volcanic regions: Comparisons between shear wave splitting and surface wave noise correlations"

PI: Martha Savage, Victoria University of Wellington
Co-PIs: Bill Fry, Art Jolly, GNS Science

Contributing students: Jessica Johnson, PhD
Rob Holt, Undergraduate Assistant (current MSc student on another project)
Brook Keats, BSc Honours

June 2012

# Layman's Abstract

Volcanic eruptions are difficult to predict and new methods are being pursued to try to add to the available techniques. Recently, changes in seismic wave properties before volcanic eruptions have been observed and proposed to be used to monitor and predict volcanic eruptions. These changing properties are interpreted as caused by changes in fluid-filled cracks, which respond to changes in stress conditions and to fluid movements. We use and compare two techniques for measuring seismic wave speeds and their variation with direction (anisotropy) in the Tongariro volcanic region. Using one technique, called "shear wave splitting" or "seismic birefringence", measured on seismic waves from nearby earthquakes, we find that there was an increase in anisotropy during the 1995/1996 Mt. Ruapehu eruption sequence and at the Tongariro geothermal area after early 2001. In contrast, anisotropy decreased during the 2006/2007 period around the times of the small 2006 and 2007 eruptions. Fast directions of anisotropy rotated after the 1995/1996 eruptions and during the time of decreasing anisotropy in 2006/2007. We attribute the changes to increasing cracks during the large eruptions of 1995/1996, to a regional movement of fluids associated with the 2006 and 2007 eruptions, and to a local disruption in the geothermal field after 2001.

We also implement a new computer algorithm to extract seismic waves from background seismic noise collected around Mt. Ruapehu. We use these waves to compute the isotropic and azimuthally dependent seismic velocity of the volcano and its surroundings. We find time-variable results that can constrain models of the evolution of the 2006 eruption. We compare these results to the above discussed shear wave splitting measurements of anisotropy. These techniques provide substantial steps toward our ultimate goal of eruption early-warning based on near-real time seismic tomography.

## Contents

**Technical Abstract**

We used data from GeoNet and past portable deployments of seismometers to determine seismic anisotropy from shear wave splitting in the Tongariro region and to compare it to isotropic and anisotropic analysis of surface waves generated by continually occurring seismic noise.

Seismicity generated from the Erua earthquake cluster (a consistently active area of seismicity about 20 km to the west of Mount Ruapehu) over the last 12 years was used to study seismic anisotropy in the Ruapehu region. In particular, we searched for changes associated with two minor phreatic eruptions on the 4th of October 2006 and the 25th of September 2007. The seismicity rate, magnitude of completeness, focal mechanisms and b-value of the cluster were also examined to investigate whether the characteristics of the seismicity changed over the duration of the study. The hypocenters were relocated, which revealed a westward dip in the shallow seismicity. Shear wave splitting revealed a decrease in delay time in the 2006–2007 period and a significant variation in the fast shear wave polarization in the same time period. The b-value also increased significantly from 1.0 ± 0.2 in 2004 to a peak of 1.8 ± 0.2 in 2007, but no other parameters were found to vary significantly over this time period. We attribute these changes to an increase in pore-fluid pressure in the Erua region due to fluid movement and suggest that this fluid movement may be associated with the eruptions in 2006 and 2007.

We applied a simplified two-dimensional tomographic inversion of recorded delay times of shear wave splitting and a spatial averaging of fast direction of anisotropy to data from temporary seismic deployments in the Tongariro Volcanic Centre in order to identify regions of changing seismic anisotropy. We observed a region of strong anisotropy (>0.025 s/km greater than the surrounding area) centered on Mt. Ruapehu in 1995, the time of a major magmatic eruption. This is interpreted to be due to an increase in fluid-filled fractures during the eruption. We also observed strong anisotropy (~0.018 s/km greater than the surrounding area) and a change in fast direction (~80°) at Mt. Tongariro in 2008 and examined the temporal evolution of this anomaly using clusters of earthquakes and permanent seismic stations in operation since 2004. This anomaly is attributed to a change in the geothermal system. A pronounced and unchanging feature was observed at Waiouru, even when the source and receiver locations differ. We therefore conclude that the transient features of strong anisotropy associated with volcanic and geothermal activity detected with this method are also robust.

Under funding from EQC grant 10/600, we have implemented an algorithm to invert ambient noise data for the isotropic velocity of Rayleigh waves. We also use this algorithm to solve for the azimuthal variance in wave speed. Since Rayleigh wave velocity depends on shear wave speeds, its analysis is complementary to the anaylsis of shear-wave splitting. An important side product of our method is the ability to model static Vs and Vs changes over very short time scales, making an advance toward the ultimate goal of near-real time monitoring based on seismic tomography. We applied this method to model changes in anisotropy generated during the 2006 eruption at Mount Ruapehu and compared it to the shear wave splitting measurements.

## Relation to other projects

This was the second of a series of proposals led by PI Martha Savage to use repeating seismic sources and borehole seismometers to monitor changes in seismic anisotropy and other seismic properties on Mt. Ruapehu Volcano. Two were funded by the Earthquake Commission and one by the Marsden Fund. The first project, No. 08/546, was focussed on creating a background static understanding of seismic anisotropy and specific velocity paths through examining repeating earthquakes and controlled source explosions. It funded a borehole installation at the Chateau observatory on the northwestern side of Ruapehu volcano, and a five-station portable network to record the Waiouru swarms, completion of an automatic analysis code for shear wave splitting, and part of the costs of detonating explosions in Lake Moawhango. Project BI 10/603, the subject of this report, funded us to retrieve and archive past portable deployments and to use them and recent data to analyse shear wave splitting and compare it to seismic noise analysis of surface waves. After this project was funded by the Marsden Fund to install a second borehole seismometer and to carry out a three-year project studying Ruapehu and six other volcanoes around the world. The purpose of the Marsden project is to study magma movement and time varying stress and seismic properties. Additionally, EQC project 10/600 "Near real-time seismic tomography on active volcanoes: Application development for eruption early warning systems" funded Co-PI Bill Fry to develop a new methodology for rapid determination of surface wave velocities from seismic noise.

PhD student Jessica Johnson received a scholarship from Victoria University and also received some funding from this grant to retrieve and archive the past datasets. She used the data in a chapter in her thesis that was published this year in Journal of Volcanology and Geothermal Research.

Honours student Brook Keats worked on this project for his Honours thesis, which was completed in 2010. This grant paid for half a summer scholarship that allowed him to rewrite the thesis as a journal article that was published in Geophysical Research Letters last year.

Undergraduate student Rob Holt was paid as an assistant to determine S arrival times and calculate shear wave splitting for the Ruapehu region. He is currently working on his MSc thesis on a different project, funded by the Evison Scholarship and by EQC to study the aftershocks of the Darfield earthquake.

## Fulfilment of Objectives:

There were two main objectives, which we discuss below along with their results.

From the proposal:

**"The first objective** is to manually re-evaluate the splitting measurements on the GeoNet stations on Ruapehu during the weeks leading up to the 2006 eruption to determine if more subtle variations are resolvable in the splitting data. We will also manually re-evaluate splitting around the 2007 eruption and for selected time periods to see if the smaller background variations observed with the noise analysis correlate with splitting changes"

We have completed this objective and more. PhD student Jessica Johnson gathered together all the data from the past portable deployments at Mt. Ruapehu and they are now on secure storage at Victoria University, and they have been given to GNS Science. We have published a paper (Johnson et al., 2012) using this work. We also hired undergraduate Robert Holt to carry out the splitting measurements around the time of the 2006 eruption, which are described below in the section "Comparison of splitting with cross-correlation at the time of the 2006 eruption". That comparison used earthquakes from the entire region to try to search for time variations. The results were equivocal probably because there is a strong spatial variation in anisotropy, discovered in the related project 08/546 (Johnson et al., 2011).

Because the results were uncertain we did not end up publishing them in this form. However, by concentrating our study on earthquakes in the Erua area, we were able to find a variation in anisotropy between Erua and Ruapehu as evidenced by earthquakes recorded at station FWVZ located at the Far West Tee Bar on the Whakapapa ski field. We found that there was a general change in anisotropy before the 2006 eruptions, which returned to normal soon after the 2007 eruptions. We also performed double-difference relocations on the earthquakes in the Erua region, which strongly delineated a difference between earthquakes in the TVZ proper and those outside the TVZ on the so-called "Taranaki-Ruapehu Line" Finally, changes in seismicity rate (b-values) were observed that correlated with the changes in shear wave splitting. (Keats et al., 2011).

As part of this project and also our Marsden project, Jolly has completed changes to the automated ambient noise algorithms to account for changes in the Ruapehu seismic network in 2009-10. The updated algorithms are now measuring relative velocity changes for two new broadband seismometers (including the new borehole seismometer located near the Chateau) in near-realtime. An addition, the older reference Greens functions have been applied to progressively older data sets as far back as January 2006. An analysis of older datasets is more problematic due to sparse network coverage and changes in station sensors and recording.

"T**he second objective** is to compare anisotropy measurements made with surface waves to those with shear wave splitting. We will determine anisotropy from surface waves and shear wave splitting at the same time period and at the same stations. "

As part of a collateral and linked EQC biennial grant 10/600, Co-PI Bill Fry has implemented an algorithm to invert ambient noise data for the isotropic velocity of Rayleigh waves. We also use this algorithm to solve for the azimuthal variance in wave speed. Rayleigh waves are a result of radial transmission of seismic energy. The velocity of Rayleigh waves is dependent on the shear modulus of the material that they are passing through and consequently has a high degree of sensitivity to shear wave velocity (Vs). Analysis of Rayleigh wave anisotropy is therefore complementary to the anaylsis of shear-wave splitting. An important side product of our method is the ability to model static Vs and Vs changes over very short time scales, making an advance toward the ultimate goal of near-real time monitoring based on seismic tomography.

We have successfully applied this method to model changes in anisotropy generated during the 2006 eruption at Mount Ruapehu. By optimizing our cross-correlation we are able to obtain stable interstation Green's Functions (GF) within one to two days of continuous recordings. However, our results indicate that standard multiple-filter techniques of dispersion measurement are not capable of extracting appropriate phase information from the resulting GF. We have modified a series of frequency domain multiple filters as well as application of phase-matching filters to enhance the fundamental mode Rayleigh waves in the GF, allowing stable dispersion measurements. By doing this, we are capable of measuring differences in shallow seismic anisotropy over day time-scales before and after the eruption. These results provide fundamental constraints on the physics of the rupture process by injecting temporal information regarding the change in stresses during the eruption process. We are in the process of generating a manuscript documenting these results. The manuscript will be included in the final report of Grant 10/600 and so is not presented in this report.

## Publications relating directly to this project:

**Refereed Journal Articles**

Due to copyright restrictions, the final articles cannot be included in this report. Instead, for two of the articles, the last submitted versions are included in the last section of the report:

Johnson JH, Savage MK, Tracking volcanic and geothermal activity with shear wave splitting tomography, Journal of Volcanology and Geothermal Research, 223-224, 1-10, doi:10.1016/j.jvolgeores.2012.01.017, 2012. (An early version of this paper appears as chapter 5 of Johnson's PhD thesis).

Jolly AD, Duputel Z, Fournier N, Monitoring of phreatic eruptions using Interferometry on Retrieved Cross-Correlation Function from Ambient Seismic Noise: Results from Mt Ruapehu, New Zealand. J. Volcanol. Geotherm. Res. (2010), doi:10.1010/j.jvolgeores.2010.01.010. (not reprinted for copyright reasons).

Keats BS, Johnson JH, Savage MK, The Erua earthquake cluster and seismic anisotropy in the Ruapehu region, New Zealand, *Geophys. Res. Lett.*, Vol. 38, L16315, 6 pp., doi:10.1029/2011GL049014, 2011.

**Honours thesis:**

Brook Keats: The Erua earthquake cluster and seismic anisotropy in the Ruapehu region, 2010, 60 pp. (presently Petroleum Geoscience Technician, Geological Resources Group, GNS Science).

**Related Publications discussed and included in the report for project** BI 10/603

**Journal articles:**

Johnson JH, Savage MK, Townend J, Distinguishing between Stress-induced and Structural Anisotropy at Mount Ruapehu Volcano, New Zealand, *J. Geophys. Res*., Vol. 116, B12303, 18 pp., doi: 10.1029/2011JB008308 2011.

Savage MK, Wessel A, Teanby NA, Hurst AW, Automatic measurement of shear wave splitting and applications to time varying anisotropy at Mount Ruapehu volcano, New Zealand, *J. Geophys. Res*., 115, B12321, doi:10.1029/2010JB007722, 2010.

Savage MK, Ohminato T, Aoki Y, Tsuji H, Greve S, Stress magnitude and its temporal variation at Mt. Asama Volcano, Japan, from seismic anisotropy and GPS, *Earth and Planetary Science Letters*, vol. 290, Issues 3-4, doi: 10.1016/j.epsl.2009.12.037, pp. 403-414, 2010.

**PhD thesis:**

Johnson, J. Discriminating between spatial and temporal variations in seismic anisotropy at active volcanoes, PhD Thesis, Victoria University of Wellington, 326 pp., submitted 5 May 2011 (now Postdoctoral Fellow at University of Hawaii, Hilo). The thesis is available online at: http://researcharchive.vuw.ac.nz/handle/10063/1849.

Comparisons between shear wave splitting and surface wave noise correlations for results from Mt Ruapehu.

**Progress Report**

**by Rob Holt**

Introduction:

The aim of this project is to produce shear wave splitting measurements for a series of sites around Mount Ruapehu around the time of the 2006 eruption (Oct 4) and compare them with the ambient seismic noise measurements shown in Mordret et al 2010.

Method:

Data (in the form of SAC files) for the period 01 August - 30 November 2006 were obtained from the geonet website (*magma.geonet.org.nz/resources/**quakesearch***) in the area: Lat:-40.2 to -38.3 Long: 174.4 to 176.8. Seven of the sites used in Mordret were used (DRZ; FWVZ; NGZ; OTVZ; TRVZ; TUVZ and WNVZ) and only earthquakes of magnitude 2 or greater were considered. Both the primary and secondary arrival times were picked for each set of data. Each pick was assigned a grade from 0 to 4, 0 being a very clear arrival and 4 being almost indeterminable. The automatic shear wave splitting (Savage et al. 2010) was performed using the MFAST package v1.2, which gave each measurement a grade from A to F (A being highest quality, F the lowest). The results for the changes in fast direction/crack orientation (Phi) and the time difference between the fast and slow direction (dt) were plotted using generic mapping tools software.

Results:

The results for stations FWVZ,TRVZ, TUVZ, and WNVZ all show no change in crack orientation around the time of the eruption (marked by star in fig. 1). The results for stations DRZ and NGZ showed no plot points around the time of the eruption.

Fig 1:

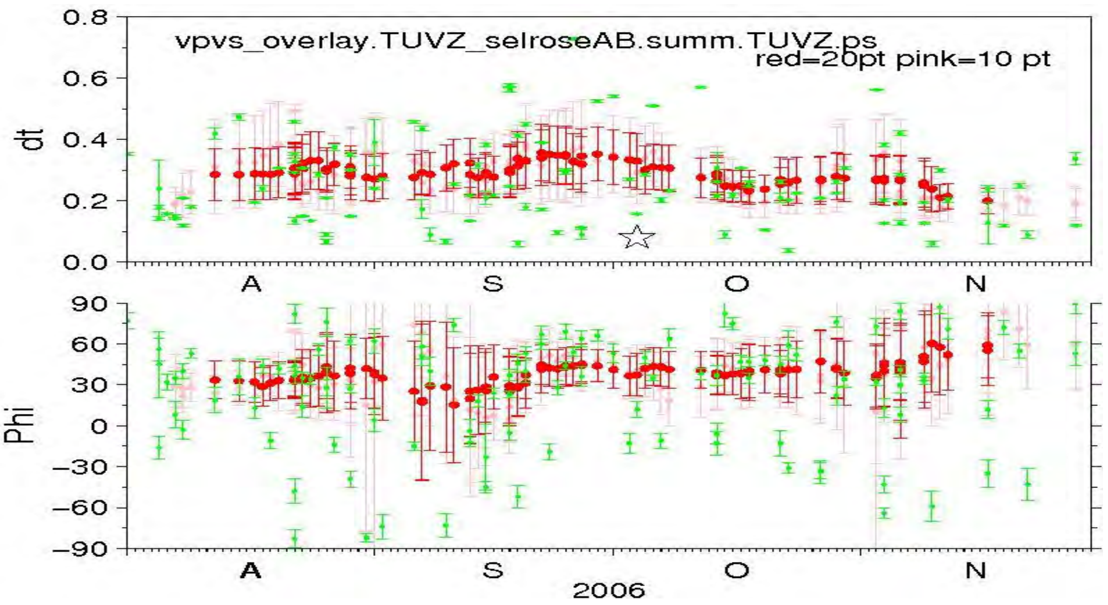


Graphs of dt and Phi for station TUVZ

Of all the stations investigated, OTVZ was the only one that produced a result comparable with those seen in Mordret et al. (2010) (see fig 2). While this result was produced using grade A and B MFAST splitting results, there were no strictures on the manual picking grades or the energy of the events. Restricting data to events with an energy of 8 or higher causes a significant reduction in plot points especially around the eruption (see fig 3).

Fig 2:

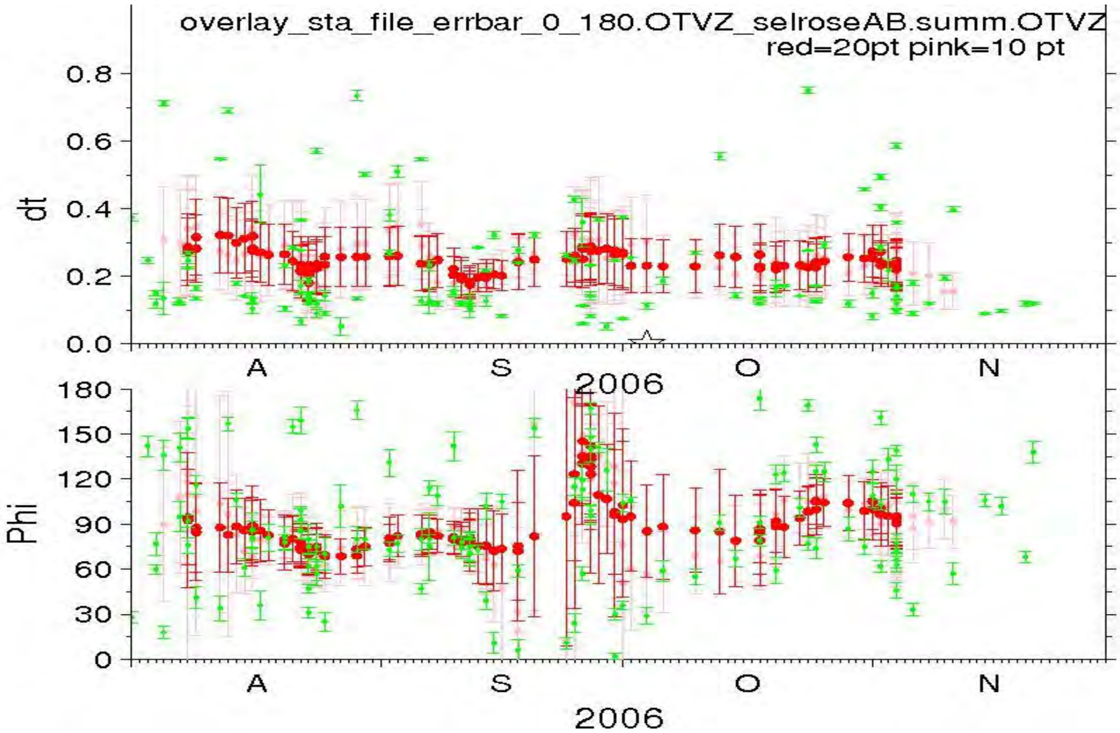


Graphs of dt and Phi for station OTVZ (no energy restriction)

Fig 3:

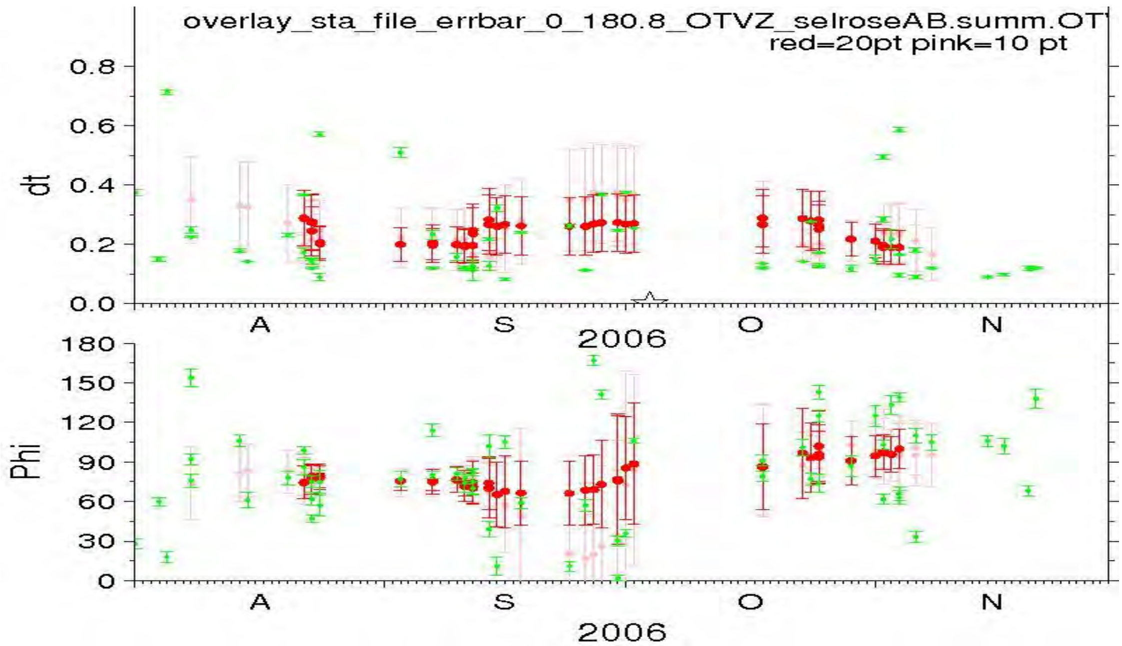


Graphs of dt and Phi for station OTVZ (energy measurements of 8 or higher)

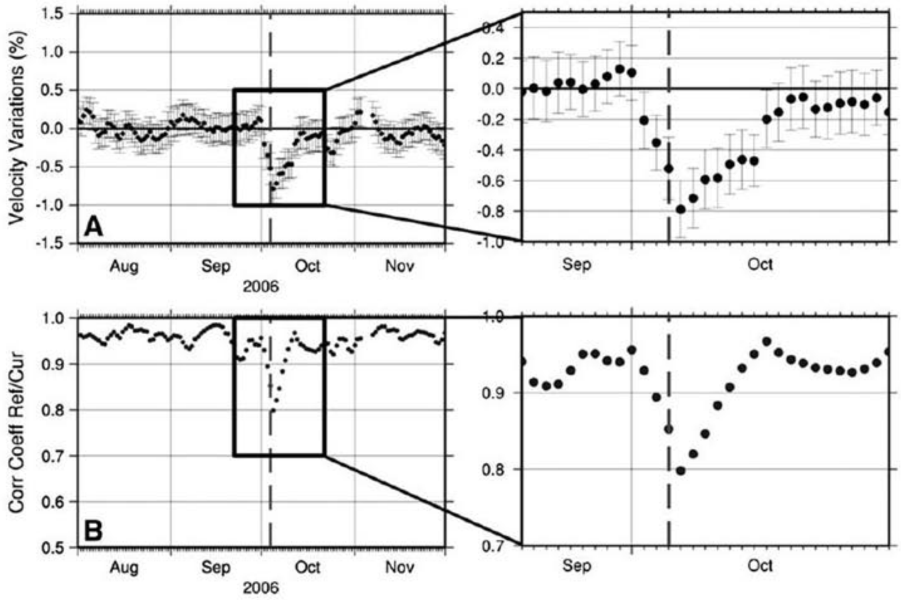


**Fig. 4.** 2006 eruption. (A) Relative seismic velocity variation $\delta v/v$ between the pair NGZ-TUVZ, the dashed gray line shows the day of the eruption. (B) Cross-correlation coefficients between the Reference CCF and the Current CCF for the pairNGZ-TUVZ. The figures on the right show the enlargement of the 22 September to 22 October period. Note the strong decorrelation which begins 3 days prior to the eruption.

Fig 4: Relative seismic velocity variation dv/v between pair NGZ/TUVZ from Mordret et al. 2010

Discussion:

Overall the results produced by cross-correlation have not been conclusively re-produced in this study. TUVZ was expected to compare well with the results from Mordret (see fig 4) as it is near the predicted position of the magma reservoir but it did not. OTVZ produced a discontinuity similar to that seen in Mordret, but this was only apparent when using low energy measurements.

References:

Mordret A, Jolly AD, Duputel Z, Fournier N, Monitoring of phreatic eruptions using interferometry on retrieved cross-correlation function from ambient seismic noise: Results from Mt. Ruapehu, New Zealand, J. Volcanol. Geotherm. Res., 191(1–2), 46–59, 2010.

Savage MK, Wessel A, Teanby NA, Hurst AW, Automatic measurement of shear wave splitting and applications to time varying anisotropy at Mount Ruapehu volcano, New Zealand, *J. Geophys. Res*., 115, B12321, doi:10.1029/2010JB007722, 2010.

# Tracking volcanic and geothermal activity with shear wave splitting tomography

Jessica H. Johnson, Martha K. Savage

*Victoria University of Wellington, School of Geography, Environment & Earth Sciences, PO Box 600, Wellington 6140, New Zealand.*

## Abstract

We apply a simplified two-dimensional tomographic inversion of recorded delay times of shear wave splitting and a spatial averaging of fast direction of anisotropy to data from temporary seismic deployments in the Tongariro Volcanic Center in order to identify regions of changing seismic anisotropy. We observe a region of strong anisotropy ($> 0.025$ s/km greater than the surrounding area) centered on Mt. Ruapehu in 1995, the time of a major magmatic eruption. This is interpreted to be due to increased fracturing during the eruption. We also observe strong anisotropy ($\sim 0.018$ s/km greater than the surrounding area) and a change in fast direction ($\sim 80°$) at Mt. Tongariro in 2008 and examine the temporal evolution of this anomaly using clusters of earthquakes and permanent seismic stations in operation since 2004. This anomaly is attributed to a change in the geothermal system. A pronounced and unchanging feature is observed at Waiouru, even when the source and receiver locations differ. We therefore conclude that the transient features of strong anisotropy associated with volcanic and geothermal activity detected with this method are also robust.

*Keywords:* Mount Ruapehu volcano, shear wave splitting, anisotropy,

*Preprint submitted to Journal of Volcanology and Geothermal Research October 14, 2011*

tomography, temporal changes, monitoring

## 1. Introduction

Shear wave splitting analysis can be used to monitor changes in rock properties (Hatchell and Bourne, 2005). However, temporal variations in seismic anisotropy measured via shear wave splitting and their interpretation are highly controversial. Among the criticisms are suggestions of observer bias in data selection (Aster et al., 1990), unsound statistical analyses (Seher and Main, 2004), misinterpretation of spatial variation (Liu et al., 2004) and lack of correlation with other stress determining factors/correlation with structural evidence (do Nascimento et al., 2004). Most of this discussion focuses on putative changes associated with large earthquakes but there have been other studies conducted on shear wave splitting around volcanoes (e.g. Volti and Crampin, 2003; Bianco and Zaccarelli, 2009; Savage et al., 2010a; Roman et al., 2011; Keats et al., 2011). Interpretation at volcanoes is often difficult due to the generally noisy waveforms and complicated interpretation of such observations when taking into account heterogeneity and complex stress regimes. Studies of shear wave splitting in volcanic environments therefore often address other stress or strain indicators in order to reduce the ambiguity in the interpretation of shear wave splitting parameters (e.g. Bianco and Zaccarelli, 2009; Savage et al., 2010a; Roman et al., 2011; Johnson et al., 2011).

In this paper we explore temporal variations of anisotropy using new methodology that minimizes the concerns previously raised. We use temporary deployments of three component seismometers around Mt. Ruapehu made in 1994, 1995, 1998, 2001, 2002 and 2008, and compare the shear wave splitting results with a benchmark of anisotropy constructed in conjunction with focal mechanism inversions and structural information (Johnson et al., 2011). Data from these deployments have been repicked and re-analyzed for shear wave splitting using the automatic algorithm, MFAST, of Savage et al. (2010b). We use an automatic algorithm to mitigate the problem of observer bias. The shear wave splitting results are then inverted using two-dimensional delay time tomography and a spatial averaging of fast directions is applied using the methods of Johnson et al. (2011). This analysis takes into account the differing earthquake and sensor locations during each of the deployments and thus enables data from different time periods to be compared. This technique reduces the uncertainty in anisotropy location that is usually present in shear wave splitting studies.

We also use clusters of earthquakes (indicated by the orange boxes in Figure 1) and permanent seismic stations to analyze the temporal variation of shear wave splitting along similar paths in order to specifically identify times of the observed changes. This technique is used so that any changes observed can be confidently interpreted to be temporal, rather than spatial artefacts of differing raypath. This method also uses MFAST to calculate the shear wave splitting parameters and the results are compared with the benchmark of anisotropy from Johnson et al. (2011) in order to refine the location of time-varying anisotropy.

The Tongariro Volcanic Centre (TVC), in the central North Island of New Zealand (Figure 1), consists of three large, historically active andesite volcanoes: Ruapehu, Ngauruhoe and Tongariro (Topping, 1974). These volcanoes are surrounded by an extensive ring plain made of fluvial, debris flow, lahar, lava, and ashflow deposits. Mount Ruapehu is a 2797 m-high andesitic stratovolcano and is the highest active volcano in New Zealand. It is the southernmost of the large active volcanoes on the North Island, which make up the Taupo Volcanic Zone (TVZ), an extending continental back-arc system resulting from the subduction of the Pacific Plate beneath the Australian Plate at the obliquely-westward dipping Hikurangi subduction zone (e.g. Walcott, 1987). Major magmatic eruptions occurred in 1945 and 1995/1996; the latter was the largest historical eruption of Mt. Ruapehu, producing a 12 km-high volcanic ash plume and lahars on the flanks of the volcano (Bryan and Sherburn, 1999). Mt. Ruapehu frequently experiences smaller phreatic and phreato-magmatic eruptions (Hurst et al., 2004), which also threaten lives and property (Johnston et al., 2000). The most recent phreatic eruptions occurred on the 4th of October 2006 and on the 25th of September 2007 (Jolly et al., 2010; Mordret et al., 2010). Mt. Ngauruhoe is also an andesite stratovolcano, which most recently erupted in 1974 and 1975 when avalanches of hot pyroclastic debris reached the base of the 900 m-high cone (Nairn and Self, 1978). Volcanic earthquakes, which suggest current active fluid movement, are frequently observed at Mt. Ngauruhoe (Jolly et al., 2011).

Eruptions of Mt. Ruapehu often occur with few or no detectable precursors, making prediction difficult (Hurst et al., 2004). For this reason Mt. Ruapehu volcano has, in recent years, been subject to several other studies of crustal seismic anisotropy using shear wave splitting analysis (Miller and Savage, 2001; Gerst and Savage, 2004) in an attempt to characterize the local stress regime. Miller and Savage (2001) measured shear wave splitting from shallow ($< 30$ km) and deep ($> 50$ km) earthquakes in 1994 and 1998 and observed a change in the dominant azimuth of fast polarization ($\phi$) spanning the magmatic eruption of 1995/1996. That study was extended by Gerst and Savage (2004), who used the same techniques and an additional deployment of three-component seismometers in 2002 to observe further changes in $\phi$.

The stress in the surrounding crust caused by the pressurized magma reservoir is thought to preferentially align randomly oriented fluid-filled microcracks and cause seismic anisotropy that is detected through shear wave splitting (e.g. Crampin, 1994; Hatchell and Bourne, 2005). The changes in $\phi$ observed in both studies were interpreted as being caused by a dike-shaped magma reservoir, or system of dikes, trending NE–SW. According to this model, the magma reservoir was pressurized before the eruption, producing a local stress field different from the regional stress field. Following the eruption the reservoir was emptier and correspondingly less pressurized, so the local stress returned to that of the surrounding region. The Gerst and Savage (2004) study suggested that the later changes in $\phi$ were due to repressurizing of the reservoir in response to an increase of magma in the system. In this paper, we re-analyze the previous shear wave splitting data used by Gerst and Savage (2004) and Miller and Savage (2001) in conjunction with data previously not used for shear wave splitting analysis. Our aim is to determine whether changes in shear wave splitting parameters associated with volcanic and geothermal activity in the TVC can be reliably detected and monitored.

## 2. Data

The two techniques employed in this paper utilize most of the available seismic data that have been recorded around Mt. Ruapehu. These data come from seven temporary deployments and the permanent seismic network. Single-component and three-component data from the permanent seismic network around Mt. Ruapehu were provided by GeoNet (last accessed 17 September 2011, `http://www.geonet.org.nz`).

Fourteen three-component seismometers were deployed around Mt. Ruapehu between 28 January and 13 March 1994 by Leeds University, the University of Memphis and the Institute of Geophysical and Nuclear Science (IGNS, now GNS Science). The purpose of this deployment was to characterize the seismicity beneath Crater Lake (Hurst, 1998).

Twelve three-component seismometers were later installed around Mt. Ruapehu between September and December 1995 by IGNS to observe the 1995 eruption sequence and to act as a backup in case the permanent stations were destroyed.

Three three-component seismometers were deployed around Mt. Ruapehu between February and July 1998 by Leeds University and IGNS. The purpose of this experiment was to characterize the post-eruption background seismicity (Sherburn et al., 1999).

The START experiment was carried out between January and June 2001 by the University of Cambridge. It was designed to create homogeneous coverage over the central and northern TVC with 28 three-component seismometers for use in seismic tomography (Rowlands et al., 2005).

In 2001, seismometers around Waiouru were installed by the University of Leeds in order to characterize earthquakes in the Waiouru swarm (Hayes et al., 2004). This deployment was a smaller part of CNIPSE (Central North Island Passive Seismic Experiment), of which we use 10 three-component seismometers.

The CHanging Anisotropy at Ruapehu Mountain (CHARM) experiment was carried out by Victoria University of Wellington (VUW) and GNS Science between January and July 2002. It was designed to reoccupy the stations from the 1994 and 1998 deployments to further investigate the changes in shear wave splitting around Mt. Ruapehu (Gerst and Savage, 2004), and consisted of nine three-component seismometers.

The Spatial Anisotropy Deployment At Ruapehu (SADAR) was part of a VUW project to investigate seismic anisotropy at Mt. Ruapehu. SADAR consisted of sixteen temporary three-component seismometers, positioned around Mt. Ruapehu during 2008 to complement the permanent (GeoNet) network of fifteen three-component seismometers (Johnson et al., 2011).

In this study, P and S phases have been picked for earthquakes occurring within 100 km of the summit of Mt. Ruapehu and shear wave splitting analysis is carried out using the automated method of Savage et al. (2010b). Figure 2 displays the locations of seismometers for each of these time periods and the raypaths of the earthquakes that were recorded in the TVC. Station details are listed in Supplementary Material S1.

## 3. Method

### *3.1. Delay time tomography and spatial averaging of $\phi$*

We have used the method of two-dimensional $\delta$t tomography and spatial averaging described by Johnson et al. (2011), and applied it to data from each of the temporary deployments. This method is based on a medium-scale optimization inversion function (*lsqlin*) in MATLAB, which uses an active set method similar to that described by Gill et al. (1981). This algorithm determines a feasible initial solution by first solving the linear least-squares problem, then converging on a final solution iteratively subject to bounding constraints. The active set refers to the elements that remain within the boundary constraints with each iteration. Hence, the constraints are set so that the minimum strength could not be below 0 s/km and the maximum could not exceed the maximum $\delta$t observed for a ray path applied to one block length, i.e. $\delta\mathrm{t}_{max}/L_{min(b)}$ where $L_{min(b)}$ is the width of the smallest in the grid.

As most of the deployments were not as dense or extensive as the 2008 deployment analysed by Johnson et al. (2011), some of the parameters have had to be changed. We used the same parameters for each deployment (Table 1).

We chose to expand the whole grid (as indicated by the limits in Table 1) in order to include earthquakes further from Mt. Ruapehu because some of the deployments would have yielded too few earthquakes otherwise. The spatial averaging only uses grid squares containing more than a certain number of rays in order to obtain a reliable mean. We lowered the minimum number of raypaths that pass through a grid square to ten from the value of twenty used by Johnson et al. (2011) to ensure that the majority of the grid squares were included in the analysis, while retaining enough for a reliable mean. The minimum grid size indicates the smallest block used for the inversion and spatial averaging. We chose to keep the minimum grid size the same, at 4 km, in order to achieve higher resolution where the data permitted and we chose to use a regular grid so that the deployments could be compared. A uniform grid facilitates use of the resolution matrices in defining the regions in which the model is well resolved, rather than using the model variance as in Johnson et al. (2011). The node spacing indicates the density of points each ray is divided into. This parameter needs to be small enough that at least one node lies in each block the ray passes through, but not too small or the computation time is excessive. The grids and rays are displayed in Figure 2.

The same grid and parameters are used for the spatial averaging of fast directions. Weighting of $1/d^2$ was applied, where $d$ is the distance of the grid block in question from the station.

The two-dimensional $\delta$t tomography method works with an assumption that $\delta$t is simply additive. This is a simplification of the non-linear relationship between heterogeneous anisotropy and the observed apparent $\delta$t at the surface. This method does also not account for any potential depth dependence of anisotropy. Johnson et al. (2011) analyzed shear wave splotting parameters from nearly one thousand earthquakes that occurred in 2008 and determined that the depth dependence of anisotropy was minimal at the time. Although depth dependence was observed on 2002 (Gerst and Savage, 2004), the quantity of deep ($> 50$ km) earthquakes in all the time periods is less than 5%, and so even if changes were observed over time using deep earthquakes, they would not affect the results significantly. Johnson et al. (2011) established that the benefit from including data from deep earthquakes outweighted any discrepancies this caused with the inversions and so we also use data from all local earthquakes. Depth dependence in other regions may increase uncertainties of this method, however the approach is designed to yield a first-order estimate of spatial variations in anisotropy.

### *3.2. Shear wave splitting using clusters*

Keats et al. (2011) carried out shear wave splitting analysis on the Erua cluster (Figure 1) and identified a significant change in shear wave splitting parameters associated with the 2006/2007 phreatomagmatic eruptions of Mt. Ruapehu. These were attributed to an increase in pore-fluid pressure close to the earthquake swarm because of the orientations of $\phi$, the decrease in $\delta$t, and also because a change in $b$-value was observed. This interpretation agrees with the conclusions of Johnson et al. (2011) that anisotropy in this area is stress-controlled. Here we examine another of the clusters of earthquakes identified by Latter (1981), the Waiouru swarm (Hayes et al., 2004) (Figure 1). Using MFAST, the same automatic shear wave splitting method as used by Keats et al. (2011), we examine shear wave splitting parameters at four permanent stations and plot the results using a moving average plot similar to that used by Savage et al. (2010a).

## 4. Results and discussion

### 4.1. Delay time tomography

The results of the delay time tomographic inversions for the six temporary deployments are displayed in Figure 3 and Supplementary Material S4.The shaded regions show the area outside the resolution as defined by the diagonals of the resolution matrices (Menke, 1989).

The stability of these results were tested by 'jackknife' tests: removing random selections of earthquakes (Supplementary material S2 and S3), and checkerboard tests (Figure 3 and Supplementary material S4). The regions of good resolution are conservative estimates based on the resolution matrices and the adequately recreated features of the checkerboard tests. The main features of strong anisotropy were found to be stable and robust following jackknife inversions using 2 sets of independent data (Supplementary material S2) and 12 sets of 80% of the data chosen at random (e.g. Supplementary material S3). The locations of the strong features did not change during the jackknife tests and we therefore assume the lateral uncertainty to be $\pm 2500$ m, which is half of the grid block size. The uncertainty in the strength of anisotropy is computed to be $\pm 0.007$ km/s, the maximum deviation from the result using all the data. The deployments in 1994, 1998 and 2002 (Supplementary Material S4) had very small areas of resolution and F tests revealed that the results from these deployments did not yield models better than the null case of uniform anisotropy; we therefore concentrate on the inversions of the 1995, 2001 and 2008 deployments (Figure 3), which were significantly better than the null case.

The feature of relatively strong anisotropy ($\sim 0.013$ s/km greater than the surrounding area) just southwest of Lake Moawhango, in the Waiouru region (Figure 3, marked with **W**) appears in each of 1995, 2001 and 2008. This is a region interpreted by Johnson et al. (2011) to have anisotropy caused in part by schistose mineral alignment and aligned fractured fault zones and would therefore be unlikely to change over time.

There are other prominent features of strong anisotropy in each of the three inversions. In 2008 the main feature of strong anisotropy is close to Mt. Tongariro ($\sim 0.018$ s/km greater than the surrounding area, marked with **T**). It is not visible in 2001, despite good resolution. This was interpreted as a highly fractured geothermal area by Johnson et al. (2011). In 2001 a prominent feature of high anisotropy lies near the Erua swarm (marked with **E**). Keats (2010) investigated the $b$-value and seismicity rate of this cluster over time and found that in 2001 there was a spike in seismicity. This is unlikely to be due to the CNIPSE deployment giving temporarily higher sensitivity because the magnitude of completeness did not go down at this time and the $b$-value decreased, both of which are contrary to what would be expected if the anomaly were due to better detection. Hence, it seems instead that there was a change in the characteristics of the Erua swarm in 2001 and this is reflected in the anisotropy tomography. The main feature of anisotropy, which is the strongest out of all of the inversions at $> 0.025$ s/km splitting, is centered just to the west of Ruapehu summit in 1995, which coincided with the major eruption. The strong anisotropy at this time is probably caused by increased fracturing of the rock during the time of the eruption. This area may also be higher than average in 1994 and 1998, although the resolution is not good (Supplementary Material S4). However, it is an area of low anisotropy in 2001 and 2008.

### *4.2. Spatial averaging of $\phi$*

The results of the spatial averaging of $\phi$ for the six temporary deployments display good continuity between deployments (Figure 4). Figure 5 displays the comparison of each deployment with the 2008 deployment (Figure 4 f). Most of the average fast directions fit well, with the L1 norm fit (S) above 0.7, where

$$\mathrm{S} = \frac{\sum |\cos(\phi_{2008} - \phi)|}{N}, \tag{1}$$

where $N$ is the number of measurements being compared.

The exception seems to be the 1994 deployment (Figure 5 a), in which all of the average fast directions have a NNW orientation. This agrees with the results of Miller and Savage (2001), even though the data were completely reprocessed and included more stations and earthquakes in this study.

All of the deployments yielding data near Waiouru show a good fit in that region. Both the 1995 and 2001 spatial average maps show high differences from SADAR near Mt. Tongariro, although there is evidence of an E–W trend just west of Tongariro in 2001. This may be because the strong anisotropy and E–W orientation of $\phi$ near Mt. Tongariro that was observed in 2008 were anomalous. We examine this anomaly in more detail in the following section.

### *4.3. Shear wave splitting using clusters*

Figure 6 displays rose diagrams of shear wave splitting results from the Waiouru swarm at the permanent GeoNet stations and moving window temporal averages from the time of installation of three-component sensors (also in Supplementary Material S5). The stations close to the Waiouru swarm

(MOVZ and MTVZ) display very little scatter. Station FWVZ, the station that displayed the most significant variation using the Erua swarm (Keats et al., 2011), does not display any marked variation at the time of the eruptions using the Waiouru swarm. This observation agrees with the interpretation that the variations detected by Keats et al. (2011) were due to near-source effects and with the interpretation of Johnson et al. (2011) that the main region of anisotropy near the Waiouru swarm is governed by structural effects such as schistose mineral alignment and aligned fractures. Moreover, the stations close to Mt. Tongariro do not display significant variations with time, although the $\phi$ results are very scattered. The tomography results from Section 4.1 suggest that there was a difference in anisotropy here in 2008 compared to 1995 and 2001, but there is no evidence for such a change when using the continuous data since 2004. The fact that the stations around Mt. Tongariro do not show significant variation during the time that they have been in operation suggests the change in anisotropy occurred before 2004. Data are not available to investigate this anomaly further. However, Hagerty and Benites (2003) identified unusual low-frequency seismic events (tornillos) beneath Mt. Tongariro beginning in early 2001 and intensifying to September 2001, which is after the time of the 2001 deployments (Hayes et al., 2004; Rowlands et al., 2005). The location of the low frequency events was found to coincide with the geothermal reservoir beneath Mt. Tongariro, suggesting that there was a change in the geothermal system at this time. This change in a system with high temperature ($> 250°$C) and pressure ($> 3.5$ MPa) fluid (Hagerty and Benites, 2003) is likely to have affected the anisotropy here.

## 5. Conclusions

Using delay time tomography and spatial averaging, we have demonstrated that unchanging features of anisotropy are reliably detected, even when the source and receiver locations differ. We therefore conclude that the transient features of strong anisotropy detected with this method are also robust. Features of anisotropy changed in relation to volcanic and geothermal activity, the most pronounced result being the strong anisotropy centered on Mt. Ruaphu at the time of the major magmatic eruption in 1995. We conclude that using an automated shear wave splitting analysis and carrying out delay time tomography and spatial averaging of shear wave splitting parameters can minimize the problem of misinterpreting spatial variations as temporal variations.

While the methods described in the paper can be used on sparse networks, the uncertainties associated with it increase due to lack of crossing rays and so it is not practical unless there is a dense permanent network. This method would also not be employable as a real-time monitoring tool because the inversion requires raypaths spanning the whole area of investigation. Therefore the results are averaged over the time of the deployment. A potential near-real time technique could use temporally moving windows, as long as the permanent network was well populated with both earthquakes and stations.

Investigation of shear wave splitting using clusters of earthquakes has been shown to be a robust way of monitoring temporal changes (Keats et al., 2011). This method is more adaptable to near-real time monitoring because measurements can be carried out as long as there are earthquakes in the cluster. However, using a cluster of earthquakes creates some scatter in the shear wave splitting parameters, which could be because of slight variations in earthquake location and source mechanism. Therefore statistical tests would have to be carried out to ensure the significance of any changes observed, which may impede real-time operation.

## 6. Acknowledgements

We gratefully acknowledge funding and support for this research received from the Earthquake Commission (EQC), the New Zealand Marsden Fund, the Foundation for Research, Science and Technology and a Victoria University of Wellington PhD Scholarship.

We thank Mark Henderson, Art Jolly and students at Victoria University of Wellington for field assistance and appreciate the help of Rob Holt and Denise Fernandez with phase picking. We gratefully acknowledge GeoNet (http://www.geonet.org.nz), a collaborative project funded by EQC and operated by GNS Science, for providing earthquake data used in this study. We are particularly grateful to Kevin Fenaughty for help with extracting waveform data from the GeoNet catalog and to Jürgen Neuberg and Steve Sherburn for information about past deployments.

We also thank John Townend, Steve Sherburn, Euan Smith and Graham Stuart for their helpful reviews.

## 7. Figures

Figure 1: Map of the Tongariro Volcanic Center showing seismicity during 2008. Labelled orange boxes indicate clusters of earthquakes, faults (black) are from the New Zealand active fault database [GNS Science, 2011]. Red inverted triangles show locations of permanent GeoNet seismic stations (GeoNet, last accessed 17 September 2011). The inset shows the study region (orange box) in the central North Island, New Zealand.

Figure 2: Maps of the stations (blue inverted triangles), grids and rays (red lines) used in the inversions and spatial averaging from the temporary deployment data in 1994, 1995, 1998, 2001 (START and CNIPSE), 2002 (CHARM) and 2008 (SADAR). Light grey boxes represent grid squares intersected by fewer than 10 rays and are excluded from the analysis.

Figure 3: Maps showing the results of the checkerboard tests and delay time tomography for three temporary deployments. Shaded areas indicate the estimated limit of resolution. **W** marks Waiouru, **R** Ruapehu, **T** Tongariro, and **E** Erua, for reference.

Figure 4: Maps of the spatial averaging of fast direction for the six temporary deployments. Red rose diagrams show all measurements in grid squares containing more than 10 passing rays and yellow bars indicate the mean fast direction in each grid square in which the standard deviation is less than 30° and the standard error of the mean is less than 10°.

Figure 5: Maps of the spatial averaging of fast direction for the six temporary deployments compared to the 2008 deployment. Blue bars show the fast direction for the grid squares in each time period and the background colours represent the difference between that result and the results in 2008. The S value indicates the L1 norm fit between the two deployments.

Figure 6: Rose diagrams illustrating $\phi$ and scaled by the number of measurements, and temporal moving averages of shear wave splitting results using the Waiouru swarm earthquakes as sources (white circles). Individual measurements for $\phi$ and $\delta t$ are displayed in blue and 20 point moving averages are displayed in red. The error bars indicate 95% confidence intervals and the grey bars illustrate the times of eruptions. Temporal analysis of stations not displayed here are given in Supplementary material S5.

Table 1: Parameters used in delay time tomography and fast direction spatial averaging.

Figure S2: Results from the delay time tomography (left column, from Figure 3 and Supplementary Material S4), two examples of jackknife tests and the difference between the two jackknifes (right column). Jackknife 1 was carried out using exactly half of the data chosen randomly, jackknife 2 was carried out with the other half so that jackknife 1 and 2 are mutually independent. **W** indicates Waiouru region, **R** is Ruapehu, **T** is Tongariro, and **E** is Erua for reference. Shaded areas indicate the estimated limit of resolution.

## Supplementary Material

Table S1: Stations used in past deployments.

Figure S3: Twelve examples of delay time tomography for the 1995 deployment using 80% of the data chosen randomly. The range of results are used to estimate the uncertainty in the model. Shaded areas indicate the estimated limit of resolution.

Figure S4: Maps showing the results of the checkerboard tests and delay time tomography for three temporary deployments. Shaded areas indicate the estimated limit of resolution. **W** marks Waiouru, **R** Ruapehu, **T** Tongariro, and **E** Erua, for reference.

Figure S5: Temporal moving averages of shear wave splitting results using the Waiouru swarm earthquakes as sources (white circles in Figure 6). Individual measurements for $\phi$ and $\delta t$ are displayed in blue and 20 point moving averages are displayed in red. The error bars indicate 95% confidence intervals and the grey bars illustrate the times of eruptions.

## References

Aster, R.C., Shearer, P.M., Berger, J., 1990. Quantitative measurements of shear-wave polarizations at the Anza seismic network, Southern California - implications for shear-wave splitting and earthquake prediction. Journal Of Geophysical Research-Solid Earth And Planets 95, 12449–12473.

Bianco, F., Zaccarelli, L., 2009. A reappraisal of shear wave splitting parameters from Italian active volcanic areas through a semiautomatic algorithm. Journal Of Seismology 13, 253–266.

Bryan, C.J., Sherburn, S., 1999. Seismicity associated with the 1995-1996 eruptions of Ruapehu volcano, New Zealand: narrative and insights into physical processes. Journal Of Volcanology And Geothermal Research 90, 1–18.

Crampin, S., 1994. The fracture criticality of crustal rocks. Geophysical Journal International 118, 428–438.

GeoNet, last accessed 17 September 2011. http://www.geonet.org.nz/.

Gerst, A., Savage, M.K., 2004. Seismic anisotropy beneath Ruapehu Volcano: A possible eruption forecasting tool. Science 306, 1543–1547.

Gill, P., Murray, W., Wright, M., 1981. Practical Optimization. Academic Press.

Hagerty, M., Benites, R., 2003. Tornillos beneath Tongariro Volcano, New Zealand. Journal of Volcanology and Geothermal Research 125, 151–169.

Hatchell, P., Bourne, S., 2005. Rocks under strain: Strain-induced time-lapse time shifts are observed for depleting reservoirs. The Leading Edge 24, 1222–1225.

Hayes, G., Reyners, M., Stuart, G., 2004. The Waiouru, New Zealand, earthquake swarm: Persistent mid crustal activity near an active volcano. Geophysical Research Letters 31.

Hurst, A.W., 1998. Shallow seismicity beneath Ruapehu Crater Lake: results of a 1994 seismometer deployment. Bulletin Of Volcanology 60, 1–9.

Hurst, A.W., Scott, B.J., Werner, C., Stevens, N., Cowan, H., 2004. Monitoring New Zealand volcanoes, in: Tephra, pp. 12–17.

Johnson, J., Savage, M., Townend, J., 2011. Distinguishing between stress-controlled and structural shear wave anisotropy at Mount Ruapehu volcano, New Zealand. Journal of Geophysical Research-Solid Earth In Press.

Johnston, D.M., Houghton, B.F., Neall, V.E., Ronan, K.R., Paton, D., 2000. Impacts of the 1945 and 1995-1996 Ruapehu eruptions, New Zealand: An example of increasing societal vulnerability. Geological Society Of America Bulletin 112, 720–726.

Jolly, A.D., Neuberg, J., Jousset, P., Sherburn, S., 2011. A new source process for evolving repetitious earthquakes at Ngauruhoe volcano, New Zealand. in prep. .

Jolly, A.D., Sherburn, S., Jousset, P., Kilgour, G., 2010. Eruption source processes derived from seismic and acoustic observations of the 25 September 2007 Ruapehu eruption-North Island, New Zealand. Journal Of Volcanology And Geothermal Research 191, 33–45.

Keats, B., 2010. The Erua earthquake cluster and seismic anisotropy in the Ruapehu region. Master's thesis. Victoria University of Wellington.

Keats, B., Johnson, J., Savage, M.K., 2011. The Erua earthquake cluster and seismic anisotropy in the Ruapehu region, New Zealand. Geophysical Research Letters Submitted.

Latter, J.H., 1981. Volcanic earthquakes, and their relationship to eruptions at Ruapehu and Ngauruhoe volcanos. Journal Of Volcanology And Geothermal Research 9, 293–309.

Liu, Y.F., Teng, T.L., Ben-Zion, Y., 2004. Systematic analysis of shear-wave splitting in the aftershock zone of the 1999 Chi-Chi, Taiwan, earthquake: Shallow crustal anisotropy and lack of precursory variations. Bulletin Of The Seismological Society Of America 94, 2330–2347.

Menke, W., 1989. Geophysical data analysis: discrete inverse theory. Academic Press.

Miller, V., Savage, M., 2001. Changes in seismic anisotropy after volcanic eruptions: Evidence from Mount Ruapehu. Science 293, 2231–2233.

Mordret, A., Jolly, A.D., Duputel, Z., Fournier, N., 2010. Monitoring of phreatic eruptions using interferometry on retrieved cross-correlation function from ambient seismic noise: Results from Mt. Ruapehu, New Zealand. Journal Of Volcanology And Geothermal Research 191, 46–59.

Nairn, I., Self, S., 1978. Explosive eruptions and pyroclastic avalanches from Ngauruhoe in February 1975. Journal of Volcanology and Geothermal Research 3, 39–60.

do Nascimento, A.F., Bezerra, F.H.R., Takeya, M.K., 2004. Ductile Precambrian fabric control of seismic anisotropy in the Açu dam area, northeastern Brazil. J. Geophys. Res. 109, –.

Roman, D.C., Savage, M.K., Arnold, R., Latchman, J.L., De Angelis, S., 2011. Analysis and forward modeling of seismic anisotropy during the ongoing eruption of the Soufriere Hills Volcano, Montserrat, 1996-2007. Journal Of Geophysical Research-Solid Earth 116.

Rowlands, D.P., White, R.S., Haines, A.J., 2005. Seismic tomography of the Tongariro Volcanic Centre, New Zealand. Geophysical Journal International 163, 1180–1194.

Savage, M.K., Ohminato, T., Aoki, Y., Tsuji, H., Greve, S.M., 2010a. Stress magnitude and its temporal variation at Mt. Asama Volcano, Japan, from seismic anisotropy and GPS. Earth And Planetary Science Letters 290, 403–414.

Savage, M.K., Wessel, A., Teanby, N.A., Hurst, A.W., 2010b. Automatic measurement of shear wave splitting and applications to time varying anisotropy at Mount Ruapehu volcano, New Zealand. Journal Of Geophysical Research-Solid Earth 115.

Seher, T., Main, I.G., 2004. A statistical evaluation of a 'stress-forecast' earthquake. Geophysical Journal International 157, 187–193.

Sherburn, S., Bryan, C.J., Hurst, A.W., Latter, J.H., Scott, B.J., 1999. Seismicity of Ruapehu volcano, New Zealand, 1971-1996: a review. Journal Of Volcanology And Geothermal Research 88, 255–278.

Topping, W.W., 1974. Some Aspects of Quaternary History of Tongariro Volcanic Centre. Ph.D. thesis. Victoria University of Wellington.

Volti, T., Crampin, S., 2003. A four-year study of shear-wave splitting in Iceland: 1. Background and preliminary analysis. New Insights Into Structural Interpretation And Modelling , 117–133.

Walcott, R.I., 1987. Geodetic strain and the deformational history of the north island of new zealand during the late cainozoic. Philosophical Transactions of the Royal Society of London 321, 163–181.

Table 1: Parameters used in delay time tomography and fast direction spatial averaging.

| Parameter | Value |
|---|---|
| West Longitude (°) | 174.842 |
| East Longitude (°) | 176.275 |
| North Latitude (°) | −38.819 |
| South Latitude (°) | −39.930 |
| Checkerboard grid size (km) | 9 |
| Node spacing (km) | 3 |
| Minimum number of rays | 10 |
| Minimum grid size (km) | 4 |

Figure 1
Click here to download Figure: Figure1.eps

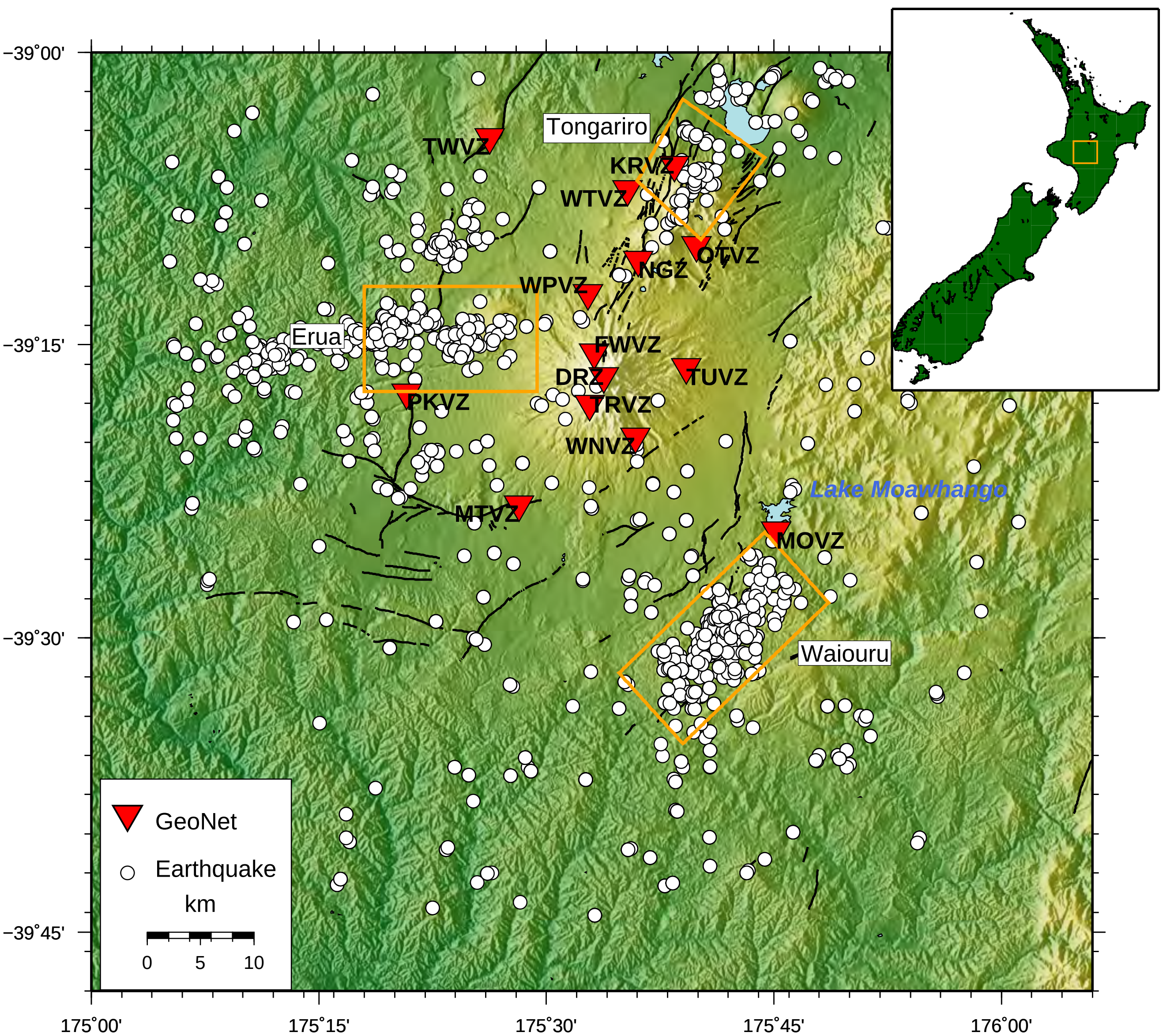

Figure 2

Click here to download Figure: Figure2.eps

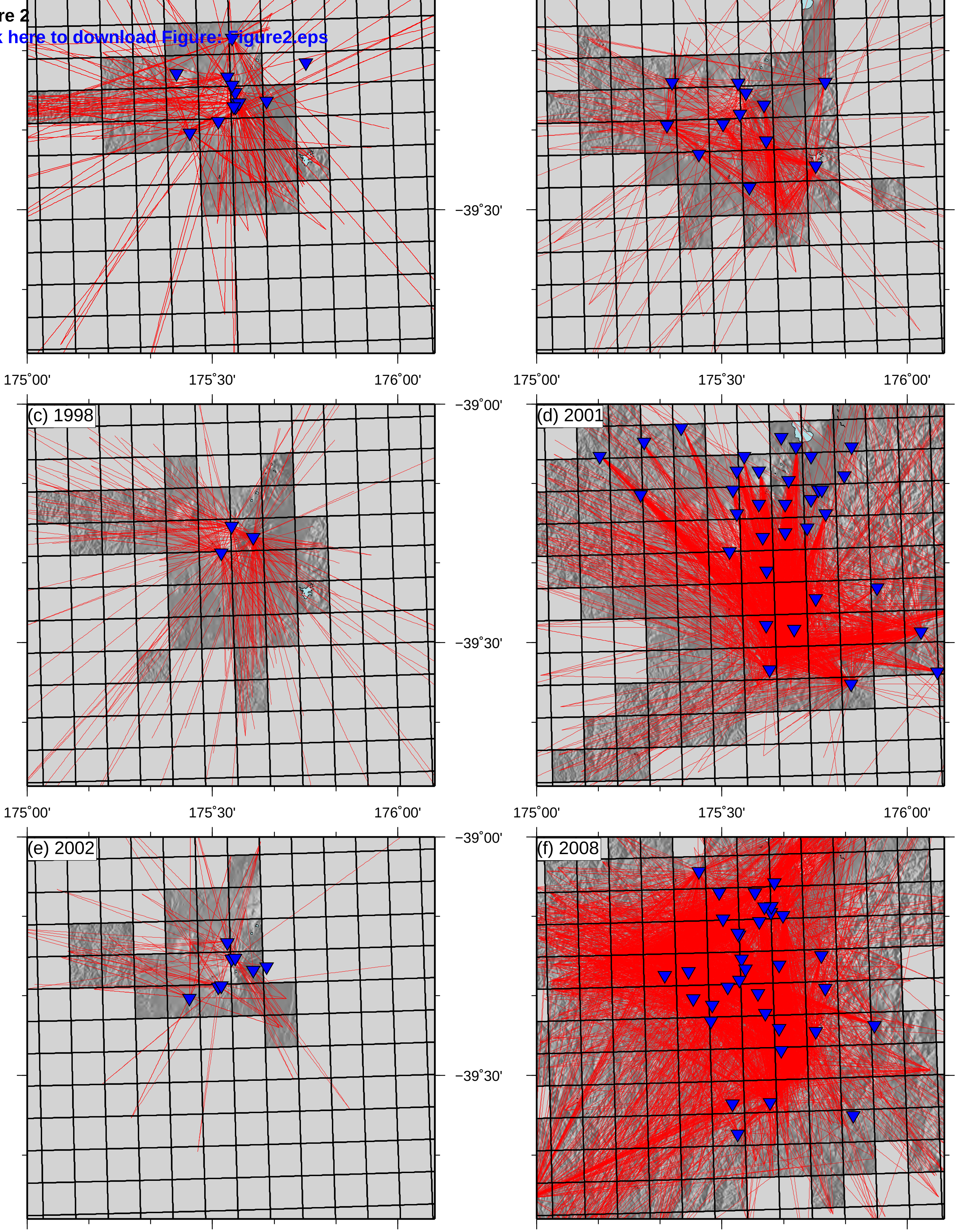

Figure 3
Click here to download Figure: Figure3.eps

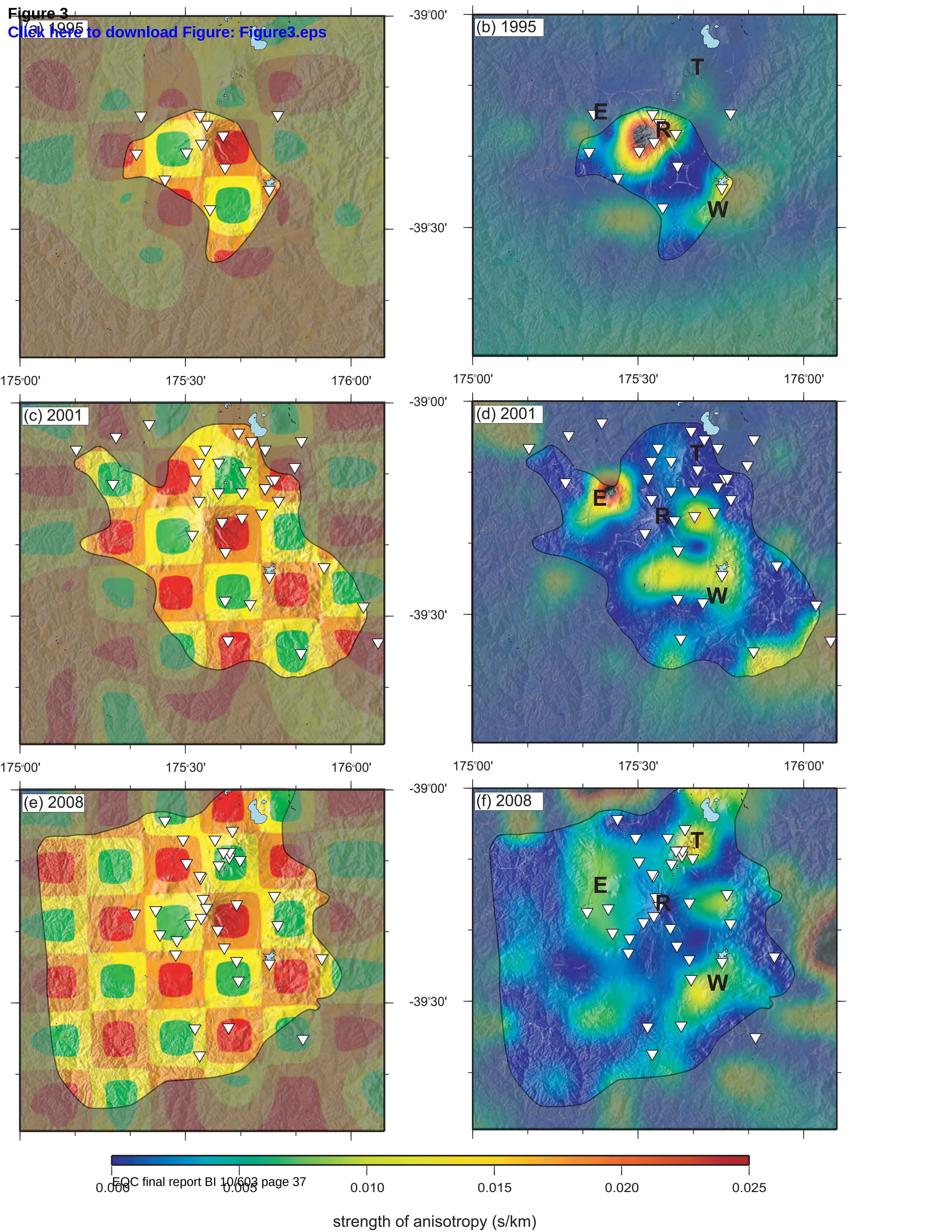

**Figure 4**

**Click here to download Figure: Figure4.eps**

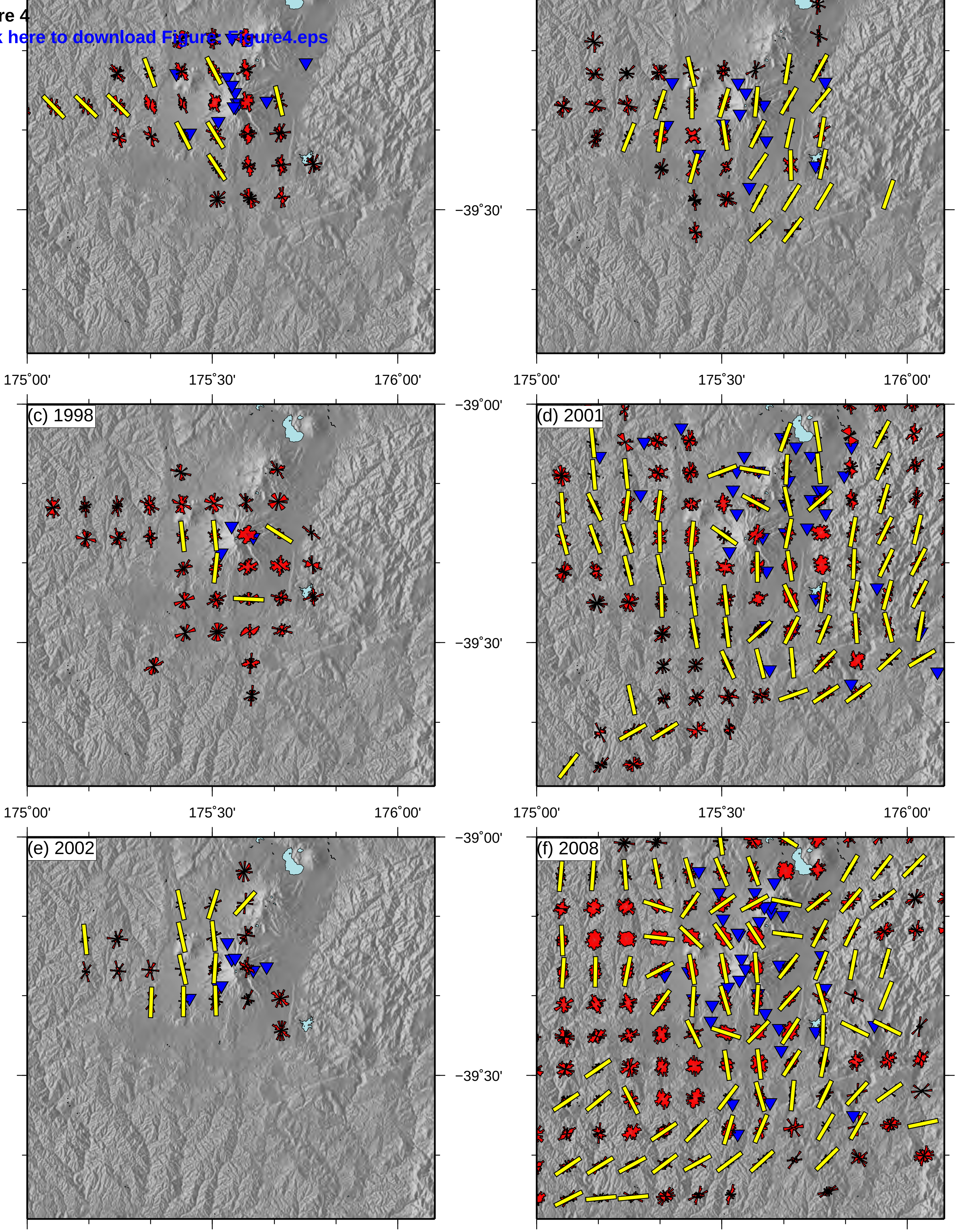

**Figure 5**
Click here to download Figure: Figure5.eps

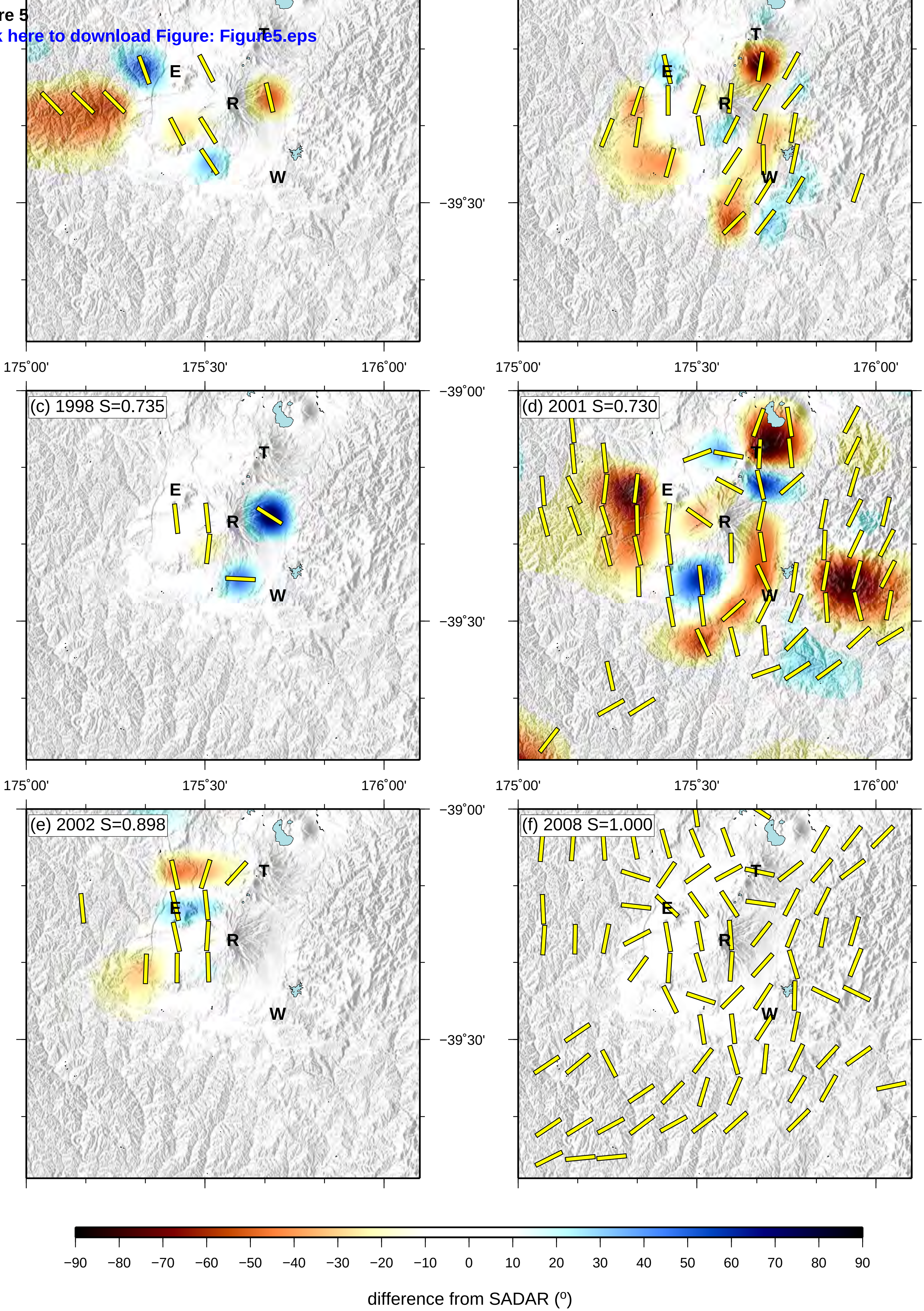

# The Erua earthquake cluster and seismic anisotropy in the Ruapehu region, New Zealand

Brook S. Keats[1,2], Jessica H. Johnson[1] and Martha K. Savage[1]

Jessica H. Johnson, Institute of Geophysics, School of Geography, Environment and Earth Sciences, Victoria University of Wellington, New Zealand. (jessica.johnson@vuw.ac.nz)

Brook S. Keats, Department of Petroleum Geoscience, GNS Science,1 Fairway Drive, Avalon 5010, PO Box 30-368, Lower Hutt 5040, New Zealand. (b.keats@gns.cri.nz)

Martha K. Savage, Institute of Geophysics, School of Geography, Environment and Earth Sciences, Victoria University of Wellington, New Zealand. (martha.savage@vuw.ac.nz)

[1]Institute of Geophysics, School of Geography, Environment and Earth Sciences, Victoria University of Wellington, New Zealand.

[2]Now at the Department of Petroleum Geoscience, GNS Science, New Zealand.

We use seismicity generated from the Erua earthquake cluster (a consistently active area of seismicity about 20 km to the west of Mount Ruapehu) over the last 12 years to study seismic anisotropy in the Ruapehu region. In particular, we search for changes associated with two minor phreatic eruptions on the 4th of October 2006 and the 25th of September 2007. The seismicity rate, magnitude of completeness, focal mechanisms and b-value of the cluster are also examined to investigate whether the characteristics of the seismicity changed over the duration of the study. The hypocenters were relocated, which revealed a westward dip in the shallow seismicity. Shear wave splitting results revealed a decrease in delay time in the 2006–2007 period and a significant variation in the fast shear wave polarization in the same time period. The b-value also increased significantly from $1.0\pm0.2$ in 2004 to a peak of $1.8\pm0.2$ in 2007, but no other parameters were found to vary significantly over this time period. We attribute these changes to an increase in pore-fluid pressure in the Erua region due to fluid movement and suggest that this fluid movement may be associated with the eruptions in 2006 and 2007.

## 1. Introduction

Understanding the temporal evolution of the stresses underlying tectonic processes remains one of the fundamental goals of geophysics. The changes in stress accompanying magma movement around volcanoes may cause changes in seismic properties, and understanding the relationship between changes in different processes is one of the ways by which we can ultimately understand volcanic activity and mitigate hazards [*Roman et al.*, 2006]. Here we examine Mount Ruapehu, an andesitic stratovolcano in the center of the North Island of New Zealand at the southern end of the Taupo Volcanic Zone (TVZ). Large magmatic eruptions have occurred several times over the last century, the largest of which were a series of phreatomagmatic–magmatic eruptions in 1995–1996 [*Johnston et al.*, 2000]. Minor phreatic and phreatomagmatic eruptions are also relatively common, the most recent of which occurred on the 4th of October 2006 and on the 25th of September 2007 [*Jolly et al.*, 2010; *Mordret et al.*, 2010].

A shear wave in an anisotropic medium will be split into a fast and slow component, with the fast polarization $\phi$ and delay time $\delta t$. Seismic anisotropy in the Earth's crust can be caused by alignment of minerals, layering of materials, fractures or stress-aligned microcracks [*Crampin*, 1994]. An applied stress field can cause microcracks to preferentially open parallel to the maximum compressive stress, causing the medium to become seismically anisotropic. This mechanism is the only one that allows seismic anisotropy to vary on time scales that are comparible with the eruptive cycle [$\sim$ 10 years, *Department of Conservation*, 2006] [*Crampin and Zatsepin*, 1997].

Previous studies by *Miller and Savage* [2001] and *Gerst and Savage* [2004] have found that the 1995–1996 eruptions of Ruapehu were accompanied by a change in the fast direction of seismic anisotropy attributed to changes in pressurization of the magmatic system. However, *Liu et al.* [2004] demonstrated that spatial variations in seismic sources can be misinterpreted as temporal changes in anisotropy as different ray paths sample different regions of the anisotropic medium. Even though SWS analysis can be used as an indicator of stress and of fluid saturation in the crust, surprisingly few studies have been conducted on shear wave splitting around volcanoes. This is due, in part, to the generally noisy waveforms and complicated interpretation of such observations when taking into account heterogeneity and complex stress regimes. Successful studies include *Bianco et al.* [2006], who observed variations in $\phi$ and $\delta t$ before the 2001 eruption on Mt Etna, Sicily; *Savage et al.* [2010], who observed strong correlations between shear wave splitting parameters and GPS baseline length changes at Asama volcano in Japan; and *Roman et al.* [2011], who observed rotations of fast directions that correlated with rotating fault plane solutions associated with volcanic activity at Soufrière Hills volcano in Montserrat. We use seismicity from the Erua earthquake cluster, a consistently active area of seismicity about 20 km to the west of Ruapehu, to measure seismic anisotropy over the last 12 years. Restricting the location of the seismic sources (earthquakes) to a cluster minimizes these spatial variations to ensure observed changes are legitimately temporal. We compare the anisotropy with relocated hypocenters and b-values.

## 2. Data

Earthquakes from the Erua earthquake cluster were recorded on the GeoNet permanent seismic network in the Ruapehu region [`www.geonet.org.nz`]. We have defined the Erua earthquake cluster as a rectangle bounded by the latitudes 39.200°S and 39.283°S, and the longitudes 175.250°E and 175.467°E (Figure 1). A total of 283 earthquakes with local magnitude ($M_L$) greater than 2 were recorded in this area on GeoNet's national seismograph network between March 1998 and June 2010. Four stations (FWVZ, MOVZ, TWVZ and WNVZ) were selected for analysis based on their location, spatial distribution and period of operation. There were 242 crustal earthquakes at depths shallower than 40 km, and 41 deep earthquakes (70–250 km) in the Wadati-Benioff zone, created by the subduction of the Pacific plate under the Australian plate beneath the North Island of New Zealand. Due to a low velocity surface layer, incidence angles of all measurements were less than the critical angle at which S–P conversions can interfere with the waveform [*Nuttli*, 1961].

## 3. Method

The earthquakes in the Erua cluster were relocated using *hypoDD* [*Waldhauser*, 2001], a double difference earthquake relocation algorithm. The algorithm was applied to catalog phase data and differential times obtained with the Bispectrum Cross-correlation package for SEISmic events [BCSEIS, *Du et al.*, 2004]. The weightings in *hypoDD* were set so that catalog picks were weighted heavily for the initial iterations and were significantly down-weighted later, while the cross correlation times were weighted weakly at the beginning and heavily at the end. This technique constrained the relative positions without sacrificing highly accurate cross correlation data [*Waldhauser*, 2001]. The velocity model used for the relocation algorithm is from *Hurst and McGinty* [1999] (see Table S1, supplementary material). To improve azimuthal coverage of the stations for the relocations, three stations to the west of the cluster (HIZ, VRZ and WAZ) were included in the analysis (inset of Figure 1).

We used the method of shear wave splitting (SWS) analysis to obtain measurements of seismic anisotropy. An automated program developed by *Savage et al.* [2010], and based on the algorithms of *Silver and Chan* [1991] and *Teanby et al.* [2004], was used to perform all SWS measurements in this study. The program grades each measurement and marks any null measurements in which no splitting result is obtained. Only non-null results with a measurement grade of A or B and delay time smaller than 0.5 s were included. Measurements that differed substantially across filters were removed, and at most one measurement is presented for each earthquake–station pair. Refer to *Savage et al.* [2010] for details on these quality control steps.

The seismicity rate, magnitude of completeness ($M_c$), and b-value of the Erua earthquake cluster were examined with time using *ZMAP* [*Wiemer*, 2001]. The magnitude of completeness is calculated for the whole catalog using the Maximum curvature method. The uncertainty on $M_c$ was calculated using 100 bootstrap calculations. A catalog of events with $M_L \geq 2$ was used to calculate a moving b-value with time. The b-value was calculated using the maximum likelihood method and plotted against time using a window of 40 events and a five event overlap (Figure 2). The uncertainty on the b-value was also calculated by bootstrapping.

## 4. Results

### Earthquake Relocation

Using *hypoDD*, 87% of the earthquakes in the catalog were relocatable (Figure 1). Average hypocenter uncertainties were 44.6 m, 47.0 m and 109.9 m in the x, y and z directions respectively calculated with the singular value decomposition (SVD) method.

Relocated earthquakes in the subducted slab showed earthquake depths around 100–150 km and depth increasing to the west along the direction of the dip of the slab.

Earthquake depths within the shallow cluster gradually increased to the west. All earthquakes were shallower than 20 km on eastern side of the Raurimu fault but on the western side some were deeper than 30 km and only one was shallower than 10 km.

### Shear Wave Splitting

SWS results were calculated using deep and shallow sources at individual stations. The orientation of $\phi$ for deep events did not vary significantly with time at any of the stations analyzed [*Keats*, 2010].

The results for shallow earthquakes are displayed as red rose diagrams in Figure 1 (d). These results were more numerous and varied between stations. At FWVZ, the station operating for the longest period of time, there were considerably more SWS results than for other stations and an interesting variation in $\phi$ and $\delta t$ with time was observed (Figure 2). Around 2005 $\phi$ changed significantly and $\delta t$ also decreased. Both parameters appeared to have reverted back to their original values by mid-2007. These changes are of interest because they precede the two minor eruptions at Ruapehu in late 2006 and late 2007.

There are some apparent gaps in the data, which are due to the lack of good shear wave splitting measurements at these times. For the most part that is because the measurements were deemed nulls (signifying no splitting). The nulls have been plotted on Figure S3 (supplementary material) to illustrate the data within the gaps. Other reasons that no measurements were obtained are that there were simply fewer earthquakes at these times, or that the waveforms were noisier and so shear wave splitting measurements could not be obtained. Some of the apparent gaps are due to a combination of these factors in that if there were more nulls at a time when there were fewer earthquakes then the gaps in the data are larger.

The results at FWVZ were divided into four time periods based on the changes observed (Figure 2). These periods were statistically analyzed for significance (Table S2, supplementary material). The analysis showed a preferential orientation in $\phi$ in the first, second and third time periods following a von Mises distribution [*Davis*, 1986]. The fourth time period had no preferred orientation. The mean value of $\phi$ changed significantly at the 90% confidence level from $-36.8 \pm 18.6°$ to $46.3 \pm 10.2°$ between periods two and three before becoming more scattered in period four. This change in $\phi$ was accompanied by a decrease in $\delta t$ from $0.122 \pm 0.020$ s to $0.083 \pm 0.015$ s between the second and third time period and an increase back to $0.137 \pm 0.037$ s in the fourth time period. The moving averages in Figure 2 display an apparent increase in $\delta t$ at FWVZ before the 2006 eruption. However, this is an artefact of the moving average window as it includes data from the other time periods and so smoothes the transitions, as can be seen from the data with no moving average plotted in Figure S3 (supplementary material).

No significant variations in $\phi$ or $\delta t$ were observed at stations MOVZ, TWVZ and WNVZ using the same time periods (Figure S3, supplementary material).

### $M_c$ and b-value

The magnitude of completeness was found to be $M_c = 1.6 \pm 0.05$, so the dataset of earthquakes with $M_L \geq 2$ that was used can be considered to be complete.

For crustal earthquakes b-values typically have values of $\sim 1$ for tectonic earthquakes, though they tend to be higher in volcanic regions [*Wiemer and Wyss*, 2002]. Figure 2 shows that the b-value of the swarm changes systematically with time. B-values began to increase significantly in 2004 from $\sim 1$ up to a peak of $\sim 1.8$ at the end of 2006 before beginning to decrease again.

## 5. Discussion & Conclusions

The Erua earthquake cluster lies around the Raurimu fault, a north–south oriented normal fault that is down-thrown to the east [*Villamor and Berryman*, 2006]. Seismicity in the cluster does not however, seem to be generated from this fault, with earthquake locations distributed evenly around it. The step in shallow seismicity (Figure 1) showed shallower earthquakes on the down-thrown eastern side, indicating that the step is not due to a seismogenic structure displaced by the fault. The Raurimu fault has been interpreted to be a shallow structure ($\sim 100$ m) [*Horspool*, 2003]. It is therefore not surprising that there is no seismic expression of the Raurimu fault at depth. The shallow seismicity on the east of the Raurimu fault is typical of the TVZ. The transition in the depth of the earthquakes is likely due to the change in geothermal gradient from within the TVZ to the cooler, thicker crust outside the TVZ. The deeper seismicity to the west may be part of a system known as the Taranaki–Ruapehu line, a line of earthquakes thought to be due to high strain rates associated with the rapid change in material properties across a step in crustal thickness [*Salmon et al.*, 2011].

At station FWVZ a significant rotation of $\phi$ and decrease in $\delta t$ was observed preceding the 2006 and 2007 eruptions. Examination of the earthquakes with time showed that locations within the cluster were sufficiently random with no migration occurring (Figure 1). Small seismogenic zones within the Erua cluster also returned changing $\phi$ over time, confirming that the observed changes at FWVZ were not due to changes in the source location (Figure S4, supplementary material). *Sherburn et al.* [2009] created a catalog of earthquake focal mechanisms across New Zealand between 2004 and 2009, 31 of which were in the region of the Erua earthquake cluster. The focal mechanisms show predominant normal faulting with no obvious change in source mechanism with time.

Variations in the seismicity rate and b-values of nearby earthquake swarms were observed at Mount Ruapehu accompanying the 1995–1996 eruptions [*Hurst and McGinty*, 1999; *Hayes et al.*, 2004]. Changes in seismicity at proximal swarms have also been observed at other volcanoes around the world such as Augustine Volcano in Alaska [*Jacobs and McNutt*, 2010], and Unzen and Kuju volcanoes in Japan [*Shimizu et al.*, 1992; *Sudo et al.*, 1998]. Using the Erua cluster, we do not observe an increase in the seismicity rate in the period around the 2006 and 2007 eruptions, yet the increase in b-value beginning in 2004 indicates that the nature of the seismicity changed before and during the eruptive period with an increase in the number of low magnitude earthquakes relative to the number of high magnitude earthquakes. An increase in b-value is expected to accompany an increase in pore-fluid pressure or an increase in thermal gradient [*Jacobs and McNutt*, 2010]. An increase in pore-fluid pressure would also decrease the crack aspect-ratio [*Zatsepin and Crampin*, 1997], therefore making the rock more isotropic and hence account for the smaller $\delta t$s from the SWS results. This effect could also account for the variation in $\phi$ observed at FWVZ: In periods two and four, $\phi$ had an orientation similar to the local stress field found by *Sherburn et al.* [2009]. We therefore infer that the anisotropy was caused by stress-aligned microcracks at these times. During period three, $\phi$ changed to a significantly different orientation. The orientation of $\phi$ in period three is sub-parallel to the Raurimu fault, indicating that the stress-induced orientation of $\phi$ could have been replaced by structurally controlled anisotropy. This would not be observed at stations farther from the cluster because there was strong anisotropy local to those stations [*Johnson et al.*, 2011]. Results using deep ($>$ 70 km) earthquakes would also fail to display a change in SWS parameters because the changes occur in the crust near the hypocenters of the shallow ($<$ 40 km) earthquakes, which is unsampled when using the deeper earthquakes (Figure 1).

A similar mechanism was proposed by *Crampin et al.* [2002] to explain "90°-flips" in $\phi$. They suggest that as the pore-fluid pressure approaches the maximum horizontal stress and the crack aspect-ratio decreases, the delay times will approach zero. At this point the anisotropy becomes negative and the fast direction will flip 90° to $S_{Hmax}$. However, according to this model the anisotropy will continue to be increasingly negative with increasing pore-fluid pressure up to about 2% anisotropy. The reason that the mechanism presented in this paper differs is because we observe a transition period of several months between the two dominant fast orientations and we observe the changes in delay time in the transition periods, and stable delay times when $\phi$ is stable. If this were a "flip" mechanism, we should observe decreasing delay time with a stable fast direction until a threshold delay time and then a sudden change to a direction which is orthogonal and an accompanying increase in delay time. In general these two mechanisms are very similar in causation but have different outcomes.

Other temporal changes in SWS parameters at volcanoes have suggested that the local stress changes due to magma emplacement. *Miller and Savage* [2001], *Gerst and Savage* [2004] and *Roman et al.* [2011] observed a rotation of $\phi$ attributed to a rotation of maximum horizontal stress. *Bianco et al.* [2006] and *Volti and Crampin* [2003] both observed increasing delay times prior to volcanic eruption, suggesting increasing differential stress, rather than increasing pore-fluid pressure. We do not find evidence that either of these models are appropriate for the data presented here.

We do not see seismicity on the Raurimu fault induced by the increase in pore-fluid pressure because the fault is much shallower than the hypocenters [*Horspool*, 2003]; however, the increase in pore-fluid pressure could increase the anisotropic effect of the other faults in the area, further increasing the dominance of the structural governance of anisotropy.

*Mordret et al.* [2010] reported decreases in isotropic Rayleigh wave speed, using noise cross-correlations, between some station pairs in two-week periods at the time of the 2006 and 2007 eruptions, suggesting that cracks opened or filled with fluids around that period. The paths with the most significant Rayleigh wave speed variations did not coincide with the paths that contain the biggest decreases in delay time that we see, although it is likely that our observations have the same mechanism.

We propose that the variations in b-value, $\phi$ and $\delta t$ observed in this study were due to fluid movement associated with volcanic activity in 2006 and 2007, similar to that in 1995–1996 [*Hayes et al.*, 2004]. In this model we propose that it is the regional fluid movement that affected both the Erua earthquake swarm and the magmatic system at Mt. Ruapehu, rather than volcanic activity affecting the fluid movement in the region. This fluid movement led to an increase in pore-fluid pressure in the Erua region. The temporal changes in seismic anisotropy observed indicate that monitoring seismic anisotropy as part of an eruption forecasting system holds potential. The nature of seismic swarms near active volcanoes seems to be linked to volcanic activity and should be taken into consideration in the monitoring process.

**Acknowledgments.** We gratefully acknowledge funding and support for this research from the Victoria University Summer Scholarships scheme, the New Zealand Marsden Fund and the Earthquake Commission. We would like to thank Steven Bannister and Andreas Wessel for providing software and advice on the use of the programs, and Euan Smith, Tim Stern and John Townend for helpful discussions. We gratefully acknowledge GeoNet (`http://www.geonet.org.nz`), for providing earthquake data used in this study.

We would also like to thank the two anonymous reviewers for their insightful comments, which improved this manuscript.

**References**

Bianco, F., L. Scarfi, E. Del Pezzo, and D. Patane (2006), Shear wave splitting changes associated with the 2001 volcanic eruption on Mt Etna, *Geophysical Journal International*, *167*(2), 959–967.

Crampin, S. (1994), The fracture criticality of crustal rocks, *Geophysical Journal International*, *118*(2), 428–438.

Crampin, S., and S. V. Zatsepin (1997), Modelling the compliance of crustal rock .2. response to temporal changes before earthquakes, *Geophysical Journal International*, *129*(3), 495–506.

Crampin, S., T. Volti, S. Chastin, A. Gudmundsson, and R. Stefansson (2002), Indication of high pore-fluid pressures in a seismically-active fault zone, *Geophysical Journal International*, *151*(2), F1–F5.

Davis, J. C. (1986), *Statistics and Data Analysis in Geology*, John Wiley & Sons, Inc.

Department of Conservation (2006), Volcanoes, East Coast/Hawkes Bay Conservancy, nS0039.

Du, W. X., C. H. Thurber, and D. Eberhart-Phillips (2004), Earthquake relocation using cross-correlation time delay estimates verified with the bispectrum method, *Bulletin Of The Seismological Society Of America*, *94*(3), 856–866.

Gerst, A., and M. K. Savage (2004), Seismic anisotropy beneath Ruapehu Volcano: A possible eruption forecasting tool, *Science*, *306*(5701), 1543–1547.

Hayes, G., M. Reyners, and G. Stuart (2004), The Waiouru, New Zealand, earthquake swarm: Persistent mid crustal activity near an active volcano, *Geophysical Research*

*Letters*, *31*(19), L19,613, doi:10.1029/2004GL020709.

Horspool, N. A. (2003), Bending stress and faulting linked to the laod of Ruapehu Volcano, Honor's thesis, Victoria University of Wellington.

Hurst, A. W., and P. J. McGinty (1999), Earthquake swarms to the west of Mt Ruapehu preceding its 1995 eruption, *Journal Of Volcanology And Geothermal Research*, *90*(1-2), 19–28.

Jacobs, K. M., and S. R. McNutt (2010), *The 2006 Eruption of Augustine Volcano, Alaska*, chap. 3: Using Seismic b-Values to Interpret Seismicity Rates and Physical Processes During the Preeruptive Earthquake Swarm at Augustine Volcano 2005–2006, pp. 1–17, U.S. Geological Survey Professional Paper 1769.

Johnson, J., M. Savage, and J. Towend (2011), Discriminating between stress-controlled and structural shear wave anisotropy at Mount Ruapehu volcano, New Zealand, *Journal of Geophysical Research-Solid Earth, Submitted, Paper #2011JB008308R*.

Johnston, D. M., B. F. Houghton, V. E. Neall, K. R. Ronan, and D. Paton (2000), Impacts of the 1945 and 1995-1996 Ruapehu eruptions, New Zealand: An example of increasing societal vulnerability, *Geological Society Of America Bulletin*, *112*(5), 720–726.

Jolly, A. D., S. Sherburn, P. Jousset, and G. Kilgour (2010), Eruption source processes derived from seismic and acoustic observations of the 25 September 2007 Ruapehu eruption-North Island, New Zealand, *Journal Of Volcanology And Geothermal Research*, *191*(1-2), 33–45.

Keats, B. S. (2010), The Erua earthquake cluster and seismic anisotropy in the Ruapehu region, Honor's thesis, Victoria University of Wellington.

Liu, Y. F., T. L. Teng, and B. Z. Yehuda (2004), Systematic analysis of shear-wave splitting in the aftershock zone of the 1999 Chi-Chi, Taiwan, earthquake: Shallow crustal anisotropy and lack of precursory variations, *Bulletin Of The Seismological Society Of America*, *94*(6), 2330–2347.

Miller, V., and M. Savage (2001), Changes in seismic anisotropy after volcanic eruptions: Evidence from Mount Ruapehu, *Science*, *293*(5538), 2231–2233.

Mordret, A., A. D. Jolly, Z. Duputel, and N. Fournier (2010), Monitoring of phreatic eruptions using interferometry on retrieved cross-correlation function from ambient seismic noise: Results from Mt. Ruapehu, New Zealand, *Journal Of Volcanology And Geothermal Research*, *191*(1-2), 46–59.

Nuttli, O. (1961), The effect of the Earth's surface on the S wave particle motion, *Bulletin of the Seismological Society of America*, *51*(2), 237–246.

Roman, D. C., J. Neuberg, and R. R. Luckett (2006), Assessing the likelihood of volcanic eruption through analysis of volcanotectonic earthquake fault-plane solutions, *Earth And Planetary Science Letters*, *248*(1-2), 244–252.

Roman, D. C., M. K. Savage, R. Arnold, J. L. Latchman, , and S. D. Angelis (2011), Analysis and forward modeling of seismic anisotropy during the ongoing eruption of the Soufrière Hills Volcano, Montserrat (1996-2007), *Journal Of Geophysical Research-Solid Earth*, *116*, B03,201, doi:10.1029/2010JB007667.

Salmon, M., T. Stern, and M. K. Savage (2011), A major step in the continental Moho and its geodynamic consequences: the Taranaki-Ruapehu line, New Zealand, *Geophysical Journal International*, *186*, 32, doi:10.1111/j.1365-246X.2011.05035.x.

Savage, M. K., A. Wessel, N. A. Teanby, and A. W. Hurst (2010), Automatic measurement of shear wave splitting and applications to time varying anisotropy at Mount Ruapehu volcano, New Zealand, *Journal Of Geophysical Research-Solid Earth*, *115*, B12,321, doi:10.1029/2010JB007722.

Sherburn, S., J. Townend, R. Arnold, and L. Woods (2009), EQC Project 08/550 - Establishing a Spatiotemporal Benchmark for Ongoing Crustal Stress Monitoring in the Southern Taupo Volcanic Zone, *GNS Science Consultancy Report*, *185*, 44.

Shimizu, H., K. Umakoshi, N. Matsuwo, , and K. Ohta (1992), *Seismological observations of Unzen volcano before and during the 1990 1992 eruption*, Kyushu University Press, Fukuoka, Japan.

Silver, P. G., and W. W. Chan (1991), Shear-wave splitting and subcontinental mantle deformation, *Journal Of Geophysical Research-Solid Earth*, *96*(B10), 16,429–16,454.

Sudo, Y., et al. (1998), Seismic activity and ground deformation associated with 1995 phreatic eruption of Kuju Volcano, Kyushu, Japan, *Journal of volcanology and geothermal research*, *81*, 245.

Teanby, N., J. M. Kendall, R. H. Jones, and O. Barkved (2004), Stress-induced temporal variations in seismic anisotropy observed in microseismic data, *Geophysical Journal International*, *156*(3), 459–466.

Villamor, P., and K. R. Berryman (2006), Evolution of the southern termination of the Taupo Rift, New Zealand, *New Zealand Journal Of Geology And Geophysics*, *49*(1), 23–37.

**Table S1.** Velocity model used during earthquake relocation [after *Hurst and McGinty*, 1999]. $v_P/v_S$ is 1.73.

| Depth to bottom of layer (km b.s.l.) | P wave velocity (km/s) |
|---|---|
| 1.5 | 3.2 |
| 5.5 | 5.5 |
| 14.5 | 5.95 |
| 32.5 | 6.5 |
| halfspace | 8.1 |

Volti, T., and S. Crampin (2003), A four-year study of shear-wave splitting in Iceland: 1. Background and preliminary analysis, *New Insights Into Structural Interpretation And Modelling*, (212), 117–133.

Waldhauser, F. (2001), hypodd– a program to compute double-difference hypocenter locations, *Open file report 01-113*, U.S. Geol. Survey.

Wiemer, S. (2001), A software package to analyze seismicity: Zmap, *Seismological Research Letters*, *72*.

Wiemer, S., and M. Wyss (2002), Mapping spatial variability of the frequency-magnitude distribution of earthquakes, *Advances In Geophysics, Vol 45*, *45*, 259–302.

Zatsepin, S. V., and S. Crampin (1997), Modelling the compliance of crustal rock .1. response of shear-wave splitting to differential stress, *Geophysical Journal International*, *129*(3), 477–494.

## Figures

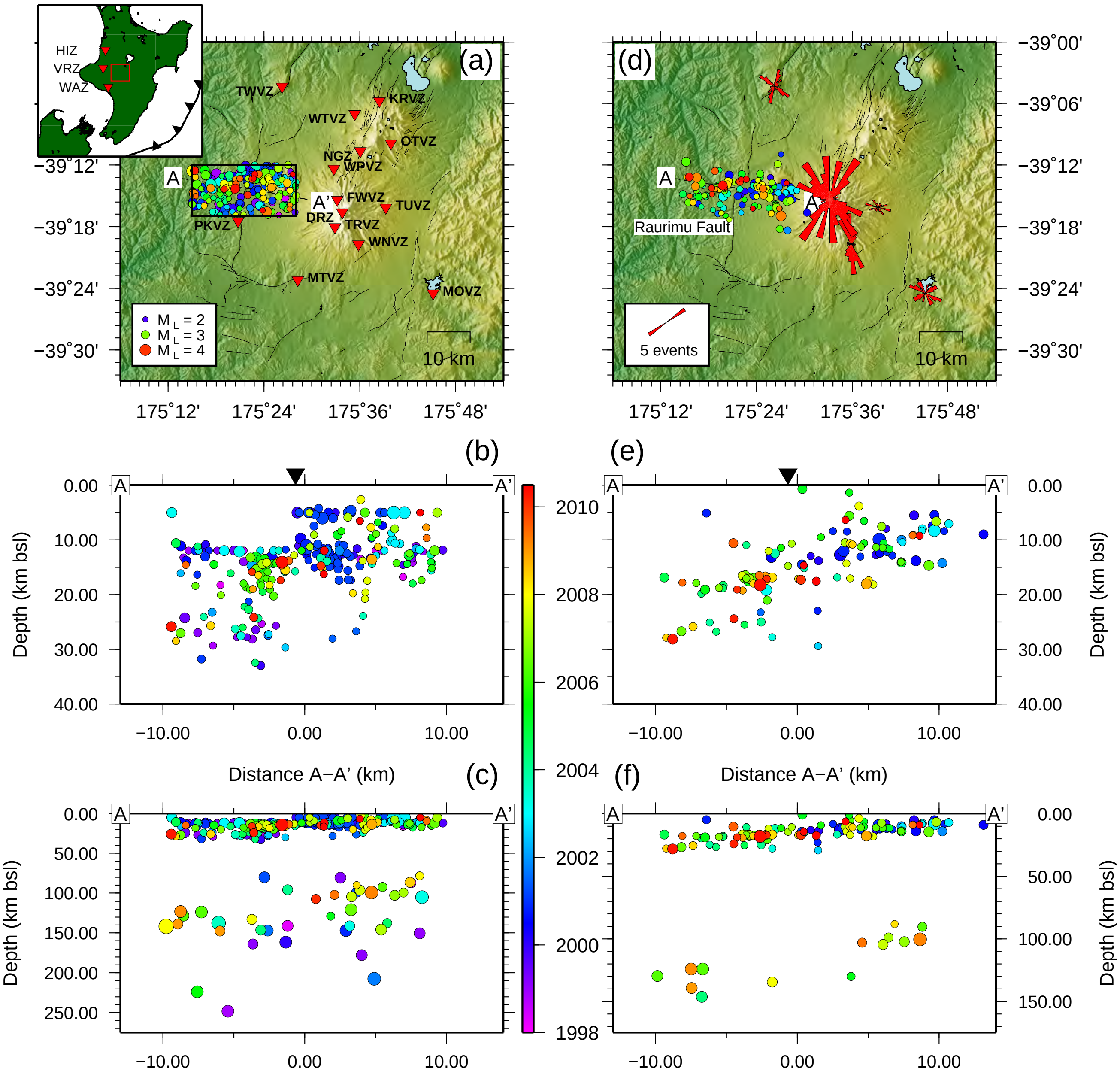
(a)
HIZ
VRZ
WAZ
TWVZ
KRVZ
WTVZ
OTVZ
NGZ
WPVZ
A
A'
FWVZ
TUVZ
DRZ
TRVZ
PKVZ
WNVZ
MTVZ
MOVZ
$M_L$ = 2
$M_L$ = 3
$M_L$ = 4
10 km
−39˚12'
−39˚18'
−39˚24'
−39˚30'
175˚12'
175˚24'
175˚36'
175˚48'
(d)
Raurimu Fault
5 events
−39˚00'
−39˚06'
−39˚12'
−39˚18'
−39˚24'
−39˚30'
(b)
(e)
Depth (km bsl)
Distance A−A' (km)
2010
2008
2006
2004
2002
2000
1998
(c)
(f)

**Figure 1.** (a) Map of the Ruapehu region showing seismic stations in GeoNet's permanent network (red inverted triangles). Catalog earthquake locations in the Erua earthquake cluster are color coded by origin time and scaled by magnitude, and active faults from GNS Science active fault database are displayed in black. Inset shows study region in New Zealand and three additional stations. (b) Cross section along A–A' showing catalog locations and depths of earthquakes in the Erua earthquake cluster shallower than 40 km. Black inverted triangle marks the location of the surface expression of the Raurimu fault. (c) Cross section along A–A' showing catalog locations and depths of all earthquakes in the Erua earthquake cluster. (d) Map of the Ruapehu region showing shear wave splitting $\phi$ results from shallow ($< 40$ km) earthquakes in the Erua cluster plotted as red rose diagrams (circular histograms) at the station that they were recorded and scaled by the number of measurements. Relocated earthquakes are color coded by origin time and scaled by magnitude. (e) Cross section along A–A' showing earthquake relocations of earthquakes shallower than 40 km. Black inverted triangle marks the location of the surface expression of the Raurimu fault. (f) Cross section along A–A' showing relocations.

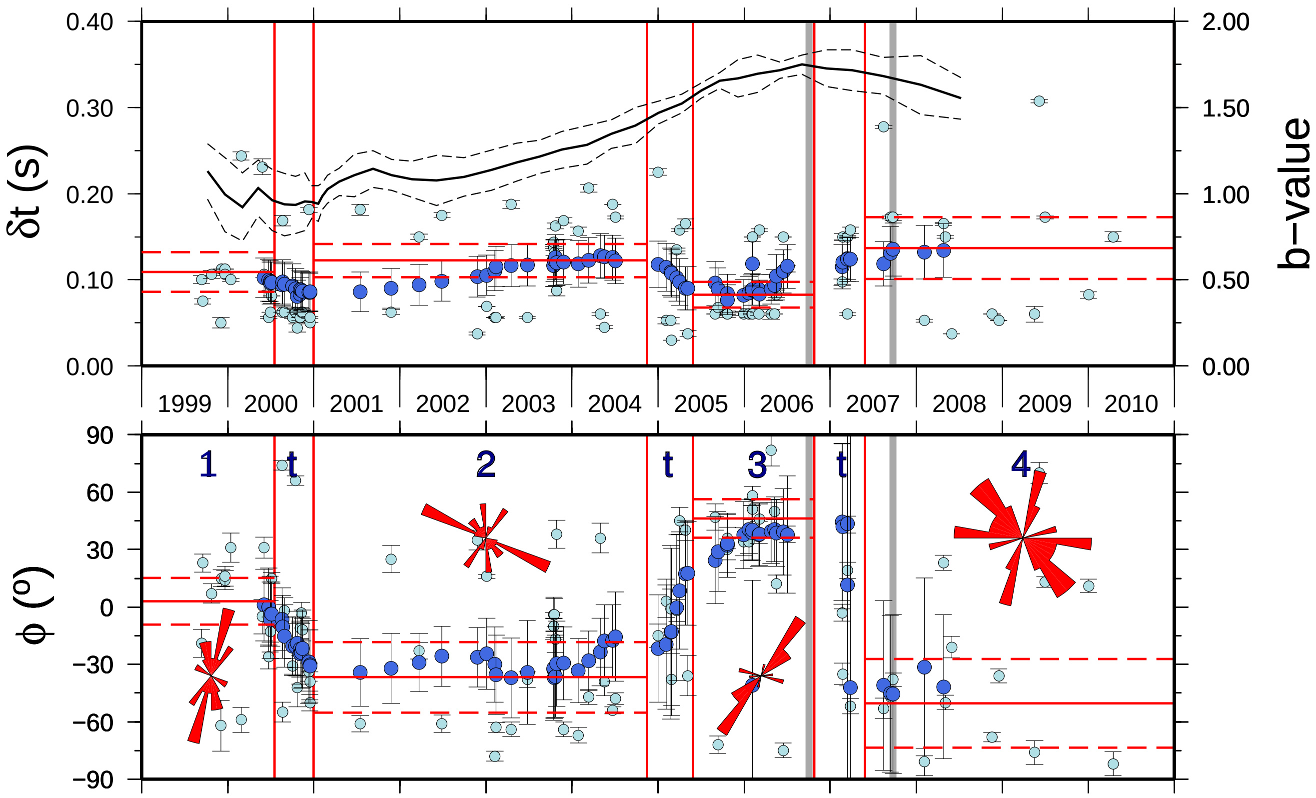


**Figure 2.** Moving average plot of fast polarization ($\phi$) and delay time ($\delta t$) using earthquakes within the Erua swarm at station FWVZ. Individual measurements for $\phi$ and $\delta t$ are displayed in light blue and 10 point moving averages are displayed in dark blue. The error bars indicate 95% confidence intervals. The four time periods, marked by the numbers 1–4, and three transition zones, marked by a **t**, are indicated with vertical red lines and the mean for each period are shown by the red horizontal bars with 90% confidence interval (dashed red lines). The times of the two phreatomagmatic eruptions that occurred are also marked with grey bars. Rose diagrams of $\phi$ are displayed in their respective time periods. The b-value for the Erua swarm catalog is also plotted against time in black at the top using a window of 40 events and an 8 event overlap. Dashed black lines indicate 95% confidence interval.

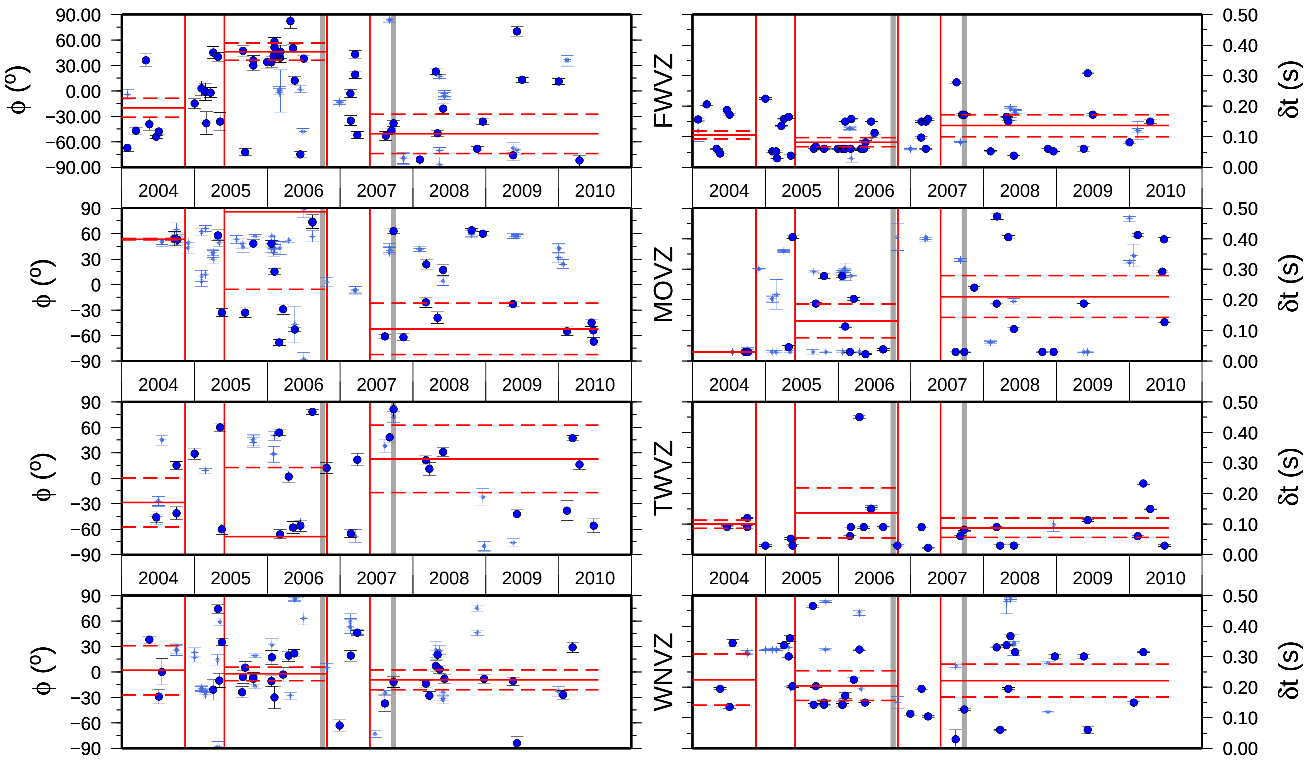


**Figure S3.** Moving average results at stations FWVZ, MOVZ, TWVZ and WNVZ from 2004 to 2011. Individual measurements for $\phi$ and $\delta t$ are displayed in dark blue and null results are in pale blue. The error bars indicate 95% confidence intervals. Grey vertical bars indicate the times of the two phreatomagmatic eruptions. Red vertical bars indicate the same time periods as those in Figure 2 and Table S2. Red horizontal bars indicate the mean values with 90% confidence interval (dashed lines) for each time period. The reason that few nulls appear on the plot of $\delta t$ at TWVZ is that they have values that are larger than 0.5 s and so are not plotted.

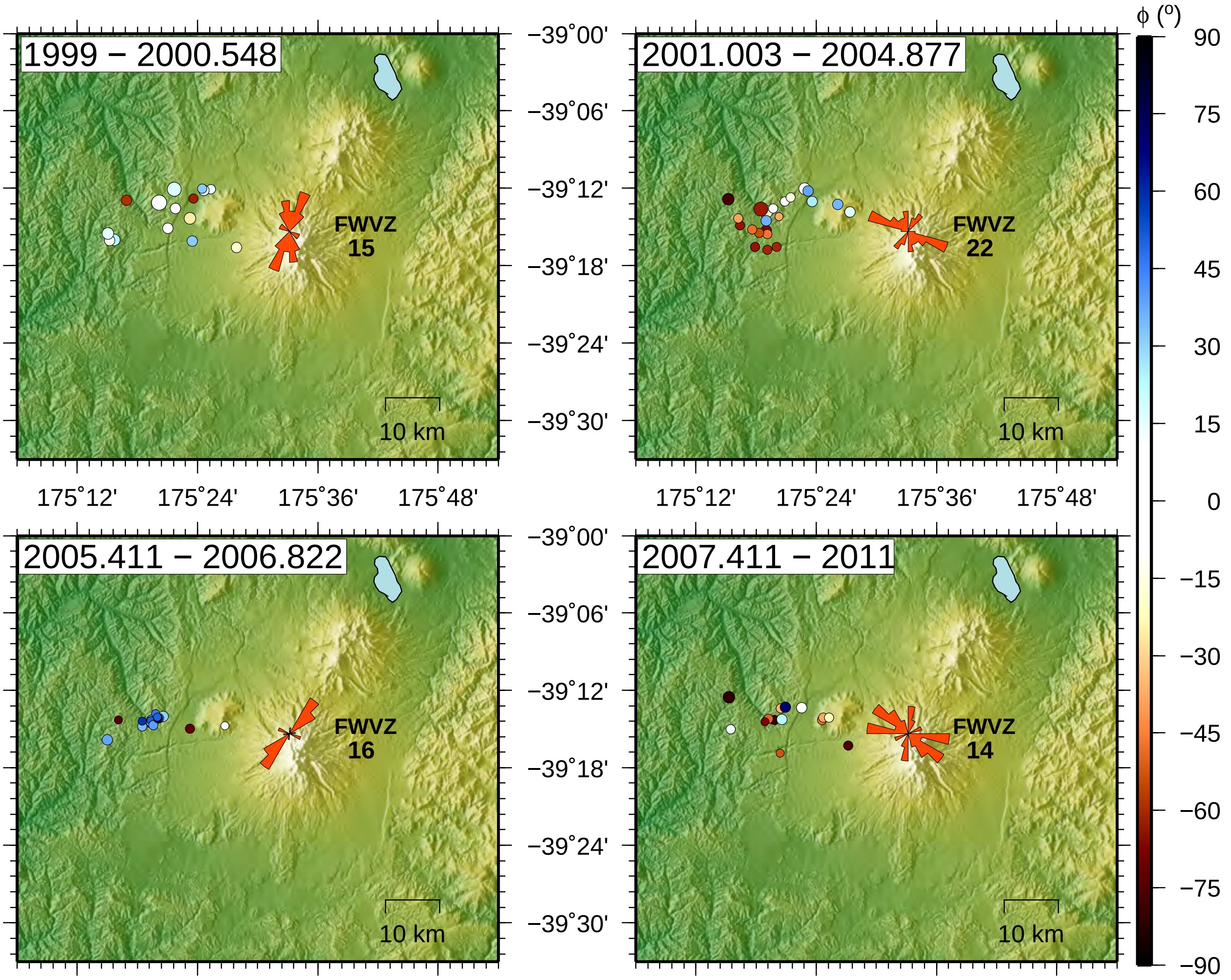


**Figure S4.** Maps of earthquake location, scaled by magnitude and colored by fast direction of anisotropy ($\phi$) recorded at station FWVZ. Panels show data for each of the time periods from in Figure 2 and Table S2. Red rose diagrams summarise the $\phi$ measurements for each time period.

**Table S2.** A summary of the statistical analysis results for each time period at station FWVZ, showing the average value and 90% confidence interval for the fast orientation $\phi$ and delay time $\delta t$. The $\bar{R}$ value is a statistical measure of dispersion for circular datasets. If this value is above a critical value ($R_{crit}$), which is a function of the number of measurements ($n$), then a preferential orientation is present for data following a von Mises distribution [*Davis*, 1986].

| Parameter | Period 1 | Period 2 | Period 3 | Period 4 |
|---|---|---|---|---|
| Time | 1999-001 – 2000-200 | 2001-001 – 2004-320 | 2005-150 – 2006-300 | 2007-150 – 2011-001 |
| $n$ | 15 | 22 | 16 | 14 |
| $\phi(°)$ | $3.0 \pm 12.1$ | $-36.8 \pm 18.6$ | $46.3 \pm 10.2$ | $-50.5 \pm 23.3$ |
| $\delta t(s)$ | $0.109 \pm 0.024$ | $0.122 \pm 0.020$ | $0.083 \pm 0.015$ | $0.137 \pm 0.037$ |
| $\bar{R}$ | 0.625 | 0.372 | 0.692 | 0.372 |
| $R_{crit}$ | 0.391 | 0.323 | 0.379 | 0.405 |